EAGLE FLAT PROJECT, HUDSPETH COUNTY, TEXAS

Jay A. Raney, Principal Investigator, E. W. Collins, Bruce Darling,
Ed Garner, M. L. W. Jackson, R. P. Langford, J. G. Paine,
Bernd Richter, B. R. Scanlon, S. J. Seni, Allan Standen,
E. G. Wermund, and Jiannan Xiang

Progress Report

Prepared for

Texas Low-Level Radioactive Waste Disposal Authority
under Interagency Contract Number IAC(92-93)-0910

by

Bureau of Economic Geology
W. L. Fisher, Director
The University of Texas at Austin
Austin, Texas 78713-7508

August 1992

QAe7664

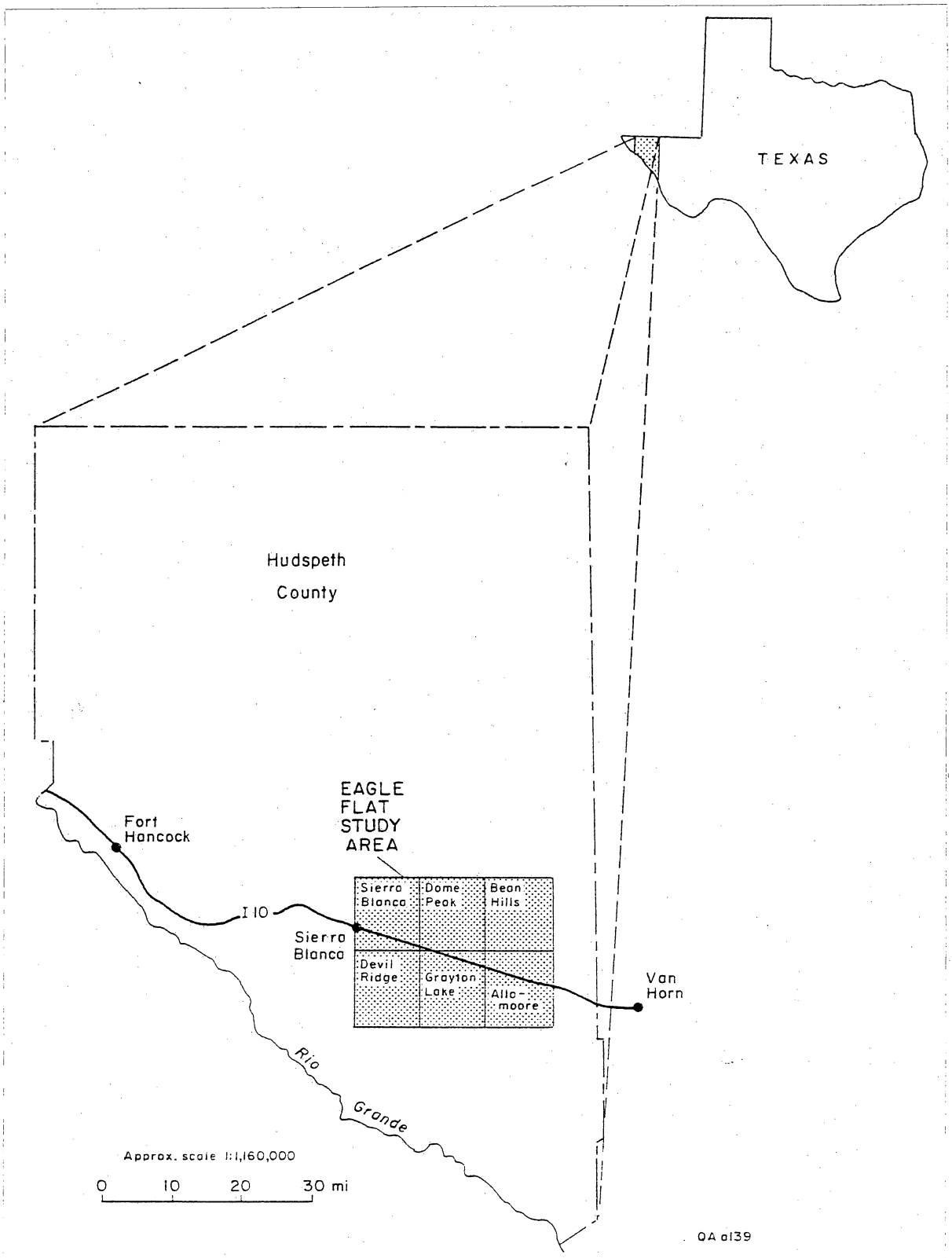

Figure 1. Map showing area designated by the Texas Legislature, the Eagle Flat study area, in Hudspeth County, Texas, and the six U.S. Geological Survey topographic quadrangle maps (1:24,000) that comprise the area.

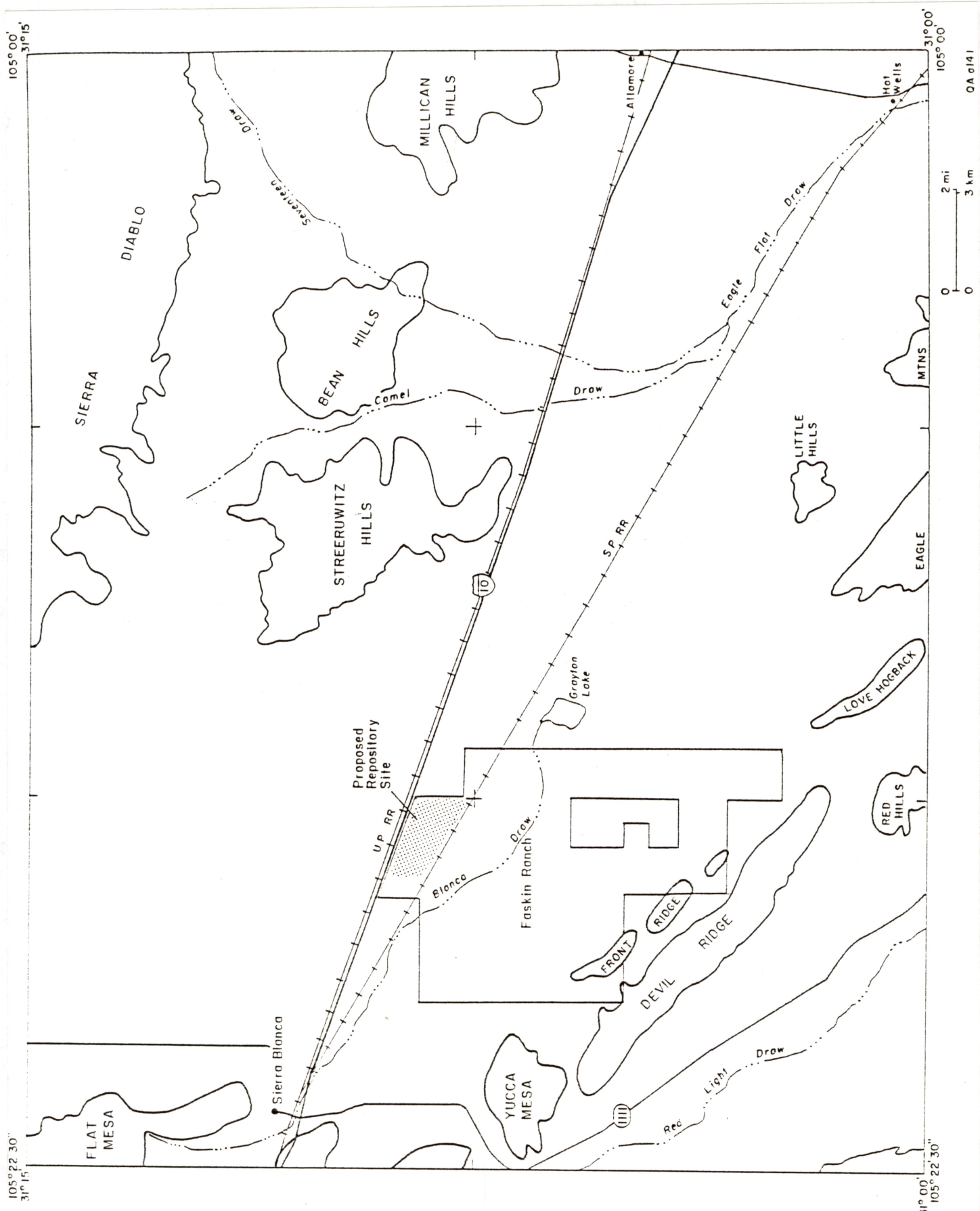

Figure 2. Map of the Eagle Flat study area showing major physiographic and cultural features, approximate boundary of the Faskin Ranch, and the currently proposed repository site.

GEOLOGIC INVESTIGATIONS

The geomorphic, stratigraphic, and structural geologic studies are designed to characterize the geologic setting of the site and region. The results of these studies are required for the license application, to support design and geotechnical studies, and to construct the hydrogeologic framework.

Various elements of the regional stratigraphy and structural setting have been described by many authors. Our studies will synthesize relevant portions of the previous work but focus on those issues that require more detailed characterization and analysis to evaluate the proposed site. Exposed bedrock geology, for example, was generally well mapped in the vicinity of the Faskin Ranch–Eagle Flat region by Underwood (1963), Albritton and Smith (1965), and King (1965). We have compiled the previous mapping on the six topographic maps (1:24,000) that cover the area designated by the Texas Legislature (fig. 1). Drilling, mapping, and geophysical studies associated with this project will add new information on the bedrock units beneath the basin-fill sediments and on the character of the basin-fill sediments themselves, particularly in the siting area.

Surficial Deposits and Basin-Fill Sediments

The proposed site at the northern Faskin Ranch (fig. 2) lies within the approximately 200-mi^2 (520-km^2) basin that is drained by Blanca Draw and its tributaries into Grayton Lake. This closed basin is contiguous with the sediment-filled valley to the east, which is drained by Eagle Flat Draw and related drainages into Lobo Valley, south of Van Horn, Texas. Understanding the surficial deposits and the underlying basin-fill sediments is important for characterizing the site, for evaluating active processes that may occur at the site, and for establishing the geologic framework for the hydrogeologic investigations. These studies also complement related studies of the soils and geotechnical properties of the near-surface deposits.

Methods of study include interpreting aerial photographs, mapping units on aerial photographs and topographic base maps, extensive field observations, and describing and sampling excavations and boreholes. The samples are being visually described and analyzed for grain-size distribution (textural analysis), carbonate content, and mineralogy. Geophysical methods, seismic reflection and refraction surveys, and paleomagnetic analyses are being conducted in concert with studies by scientists at The University of Texas at El Paso. The results of the geophysical surveys, described later in this report, are important to the stratigraphic studies of the basin-fill sediments.

Surficial Deposits and Surface Morphology

Mapping the surface morphology and surficial deposits of northern Faskin Ranch, in and around the proposed site, was one of the initial objectives of the characterization program. Geomorphic elements were mapped using aerial photographs and checked by field observation. Shape features and slopes for each geomorphic element were quantified using topographic maps. In the principal siting area, surficial deposits were mapped along traverses spaced 2,000 ft (610 m) apart to create a grid. Samples of surficial deposits were collected from shallow, hand-dug pits at depths as much as 1.6 ft (0.5 m) below the surface. The samples were collected from different depths at 13 locations to quantify textural and compositional changes with depth.

Outside the immediate area of the proposed repository, surficial deposits were mapped using both interpretations of aerial photographs and field observations made along traverses designed to cross all of the map elements visible on aerial photographs. Samples were collected from 23 locations, in addition to those collected on the proposed site, along the traverses.

The northern Faskin Ranch area can be generally divided into three geomorphic regimes, washes, wash-flank slopes, and interfluvial flats. The wide flat washes of Blanca Draw and its tributaries form a dendritic network trending east, southeast, and south through the area (figs. 3

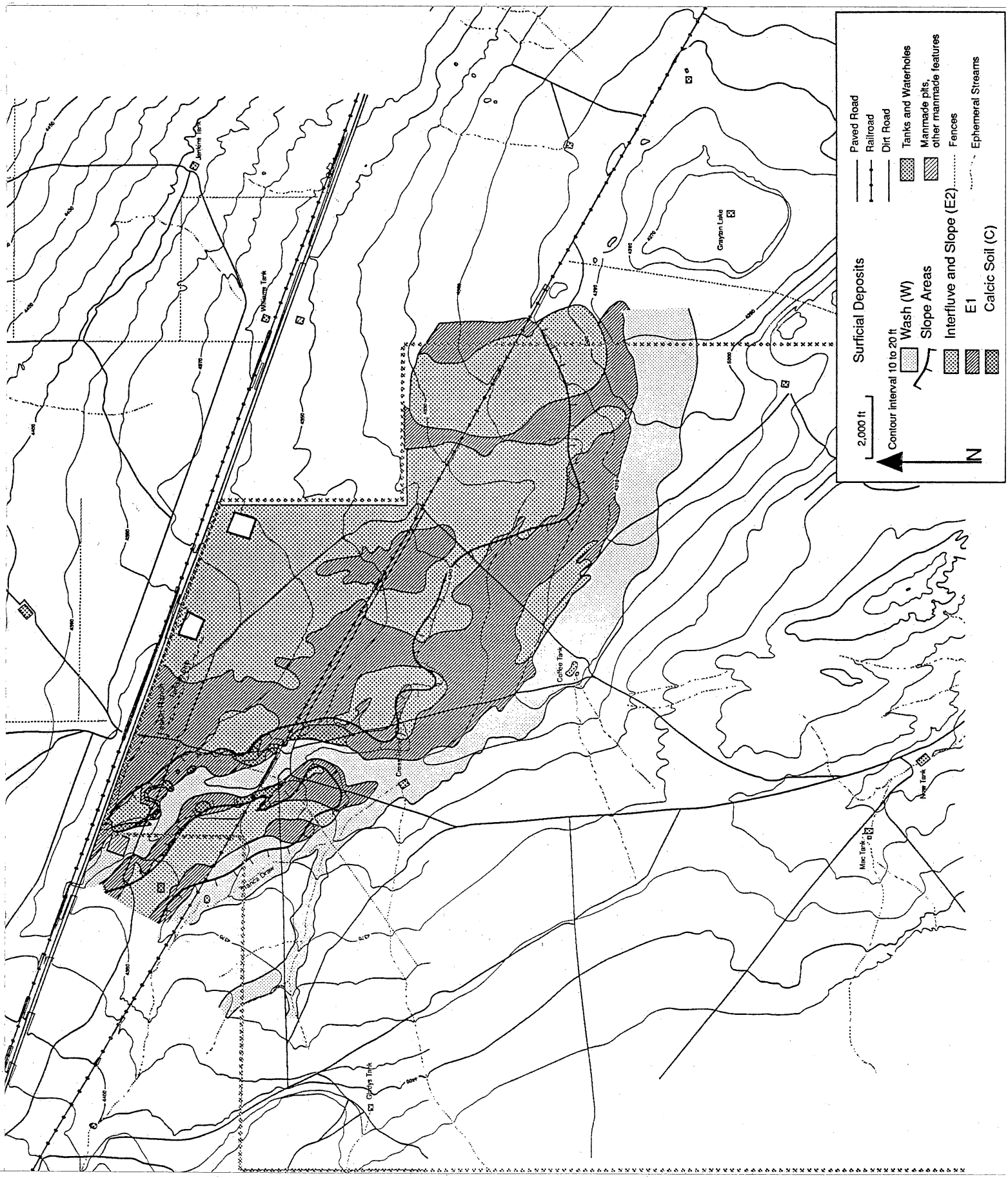

Figure 3. Map of the geomorphic elements and surficial deposits of the northern Faskin Ranch area. Hachured lines indicate slope areas. Shaded patterns show distribution of surficial deposits.

and 4). The washes are separated from intervening interfluvial flats by well-defined, wash-flank slopes (figs. 3 and 4). Washes are 200 to 1,650 ft (60 to 500 m) wide, with an average width of 950 ft (290 m; fig. 3). Washes are 7 to 35 ft (2.1 to 10 m) below adjacent interfluves and have gradients that vary from 0.0053 (28 ft per mi) in the northwest part of the north Faskin area to 0.0019 (10 ft per mi) near Coffee Tank. Wash floors are vegetated and only locally exhibit channels or other erosional or depositional features resulting from active fluvial or alluvial processes.

Washes can be subdivided into three areas according to distinct vegetation types: (1) mesquite thickets having scattered to dense stands of mesquite interspersed with grasses and other shrubs, (2) grass flats having dense patches of grass, and (3) grass flats covered with scattered grasses. Mesquite thickets are wider and more common in the lower reaches of Blanca Draw, in the southeast part of the area. The thickly vegetated grass flats form isolated patches along the margins of the washes.

Wash-flank slopes are defined by their relatively steeper slopes between the interfluvial flats and the wash bottoms (fig. 4). The slopes are locally well defined on contour maps and in many places are visible on aerial photographs. Wash-flank slopes average 790 ft (240 m) in width and have slopes averaging 0.019 (99 ft per mile). Vegetation is generally similar to that of the interfluvial flats (see next paragraph) but is less dense. The wash-flank slopes are actively eroding in some areas. The characteristic erosional features are crescentic erosional scarps, 0.3 to 1.0 ft (0.1 to 0.3 m) high, that open downslope and enclose poorly vegetated or nonvegetated fan-shaped areas in which shallow rills may be present. Sediment is evidently sapped from the scarp face, washed across the barren fan-shaped area, and deposited in grassy areas at the toes of the scarps. Sediment derived from the scarps is deposited within the adjacent parts of the washes. Erosion has also occurred along cow paths, roads, trails, and other areas subject to the activities of people or cattle.

Interfluvial flats are present over most of the northern Faskin Ranch area (fig. 3). The interfluves are low-relief, mesquite and yucca savannas that slope gently southerly, with a

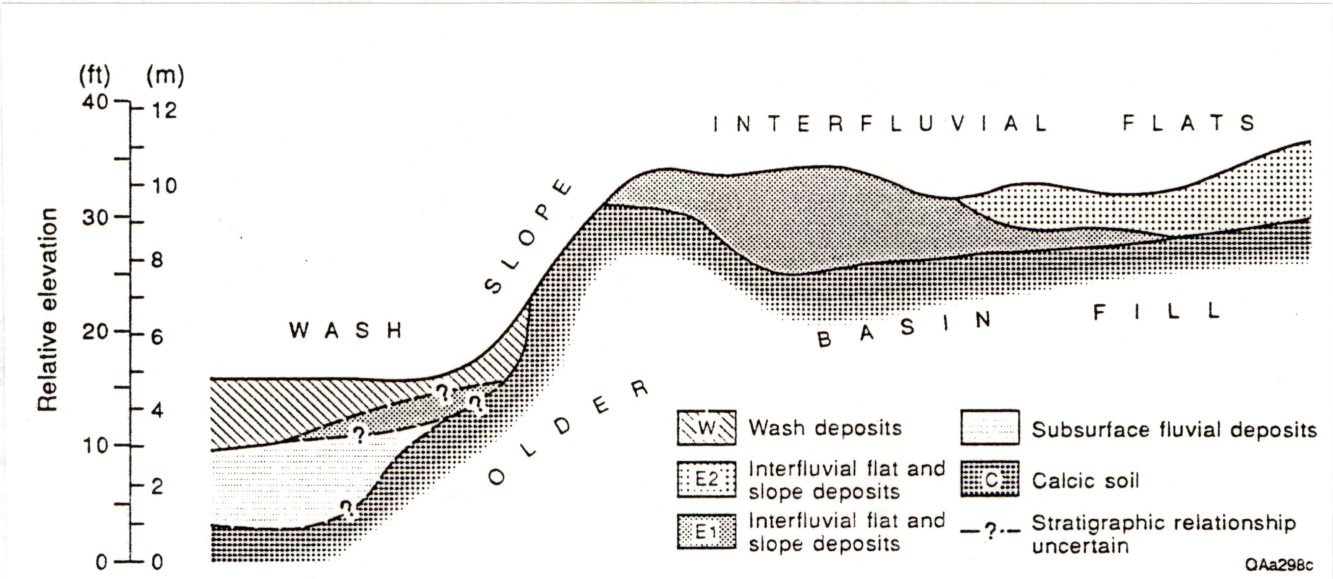

Figure 4. Schematic cross section through Blanca Draw, adjacent slope, and interfluvial flats indicating topographic expression and stratigraphy of surficial deposits. No horizontal scale.

gradient of 0.0043 (23 ft per mi), across the north part of the ranch. The interfluves are vegetated and do not exhibit channelization or erosional or depositional features resulting from fluvial or alluvial activity. Topographic maps having a 2-ft contour interval reveal a gently rolling topography that has 3- to 6-ft-high (1- to 2-m), north-elongate swells and intervening swales (figs. 4 and 5).

The floors of washes are underlain by a substrate that has a texture different from the other geomorphic elements. The wash deposits (W) are cohesive and appear to have a high silt and clay content. Grain-size analyses are pending. Pebbles are only evident along the margins of washes, where they are being eroded from flanking slopes of the washes. Internal laminations or other bedding surfaces are not commonly evident, and primary depositional features may have been destroyed by soil-forming processes. This facies appears to be the youngest surficial deposit in the northern Faskin Ranch area and is probably currently aggrading. The facies thins to a zero-edge at the margins of the washes and thickens to at least 1.6 ft (0.5 m) within the rest of the washes (figs. 3 and 4).

Two different substrates appear to underlie the interfluvial flats (figs. 3 and 4). The younger interfluvial deposits (E2) are fine-grained loamy sands with no pebbles or caliche fragments included and little evidence of soil development. The older interfluvial deposits (E1) are also fine-grained sands, but they contain pebbles and caliche fragments that are scattered across the surface of areas underlain by E1. The E2 deposits may be significantly younger than the E1 deposits because in some locations E2 overlies E1 with a sharp contact and because E1 exhibits horizons associated with clay and carbonate accumulations formed during soil development. The E1 deposits are internally somewhat variable and may be subdivided as work continues. Samples of both the E2 and the E1 deposits will be processed to measure the clay and carbonate content. The E1 and E2 units have an irregular contact, and both exhibit the rolling topography typical of the interfluvial flats (figs. 4 and 5).

Unit C underlies the E2 and E1 deposits and is exposed along wash flanks and in excavations (figs. 3 and 4). The C deposits typically contain a readily apparent calcic soil

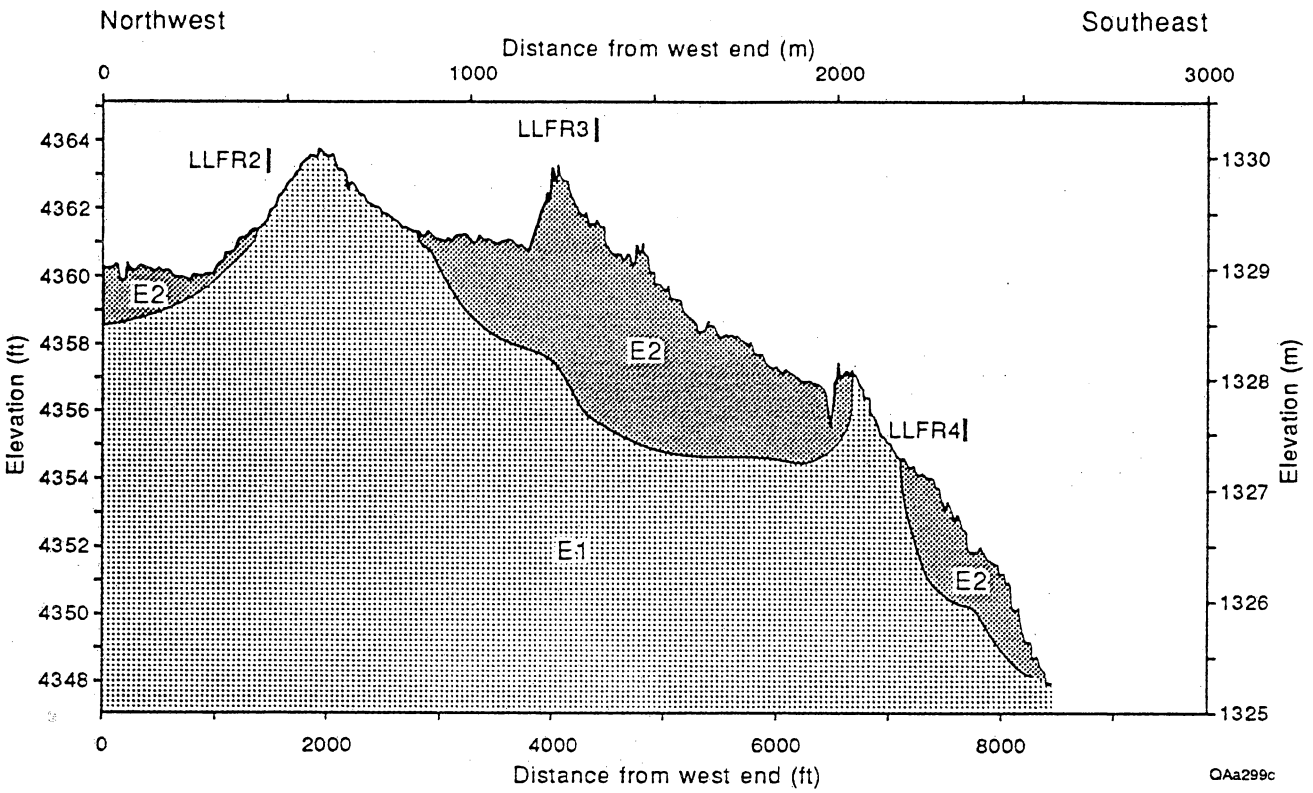

Figure 5. Detailed topographic profile across the interfluvial flats illustrating the high frequency relief on the topographic surface of the E2 deposit and the rolling topography typical of the interfluvial flats. Vertical exaggeration is about 600:1. Location of profile is along seismic reflection line LLFR1 (see fig. 16).

horizon, which is variably developed, and in some places no calcic horizon is evident. Most commonly the soil is a horizon of massive $CaCO_3$ indicative of stage III development, and locally stage IV calcretes are evident (following usage of Machette, 1985). Soils with similar stage III carbonate development in southern New Mexico and West Texas require 100,000 to 150,000 yr to accumulate (Machette, 1985), and the actual age of unit C may be much older.

The calcic soil is developed in a heterogeneous suite of materials, including sands, muddy sands, and gravels. The deposits appear to be predominantly fluvial in origin. Locally, gravel lenses and coarse sands are present below the calcic horizon. In most exposures, only the calcic horizon is exposed, and the parent material is not evident. In one borrow pit in Blanca Draw, the calcic soil is overlain by a 6.9-ft-thick (2.1-m) lens of muds, sands, and gravels having sedimentary structures indicating a fluvial origin (fig. 4). This deposit appears to underlie E1 although the stratigraphic relationship between E1 and the fluvial strata is not well exposed.

Basin-Fill Sediments

Surficial deposits at Faskin Ranch, just described, are unconsolidated to poorly consolidated Quaternary deposits of eolian, colluvial, and alluvial origin. These sediments, and an underlying sequence of similar lithologies, were deposited within a basin developed on an irregular bedrock surface. The depth of the basin-fill deposits above the bedrock in the vicinity of the proposed site at the northern Faskin Ranch, on the basis of drilling (fig. 6), ranges from approximately 160 ft (50 m) (borehole YM-5) to 680 ft (210 m) (borehole YM-17). Basin-fill deposits are being studied in surface exposures, excavations, and in samples acquired from core and auger holes at Faskin Ranch and Grayton Lake (fig. 6). In total, more than 3,000 ft (900 m) of basin-fill sediments have now been cored. The bedrock exposed in the vicinity of Faskin Ranch and sampled in boreholes is composed of Cretaceous limestones and sandstones. Tertiary igneous rocks, Paleozoic sedimentary rocks, and Precambrian sedimentary and metamorphic

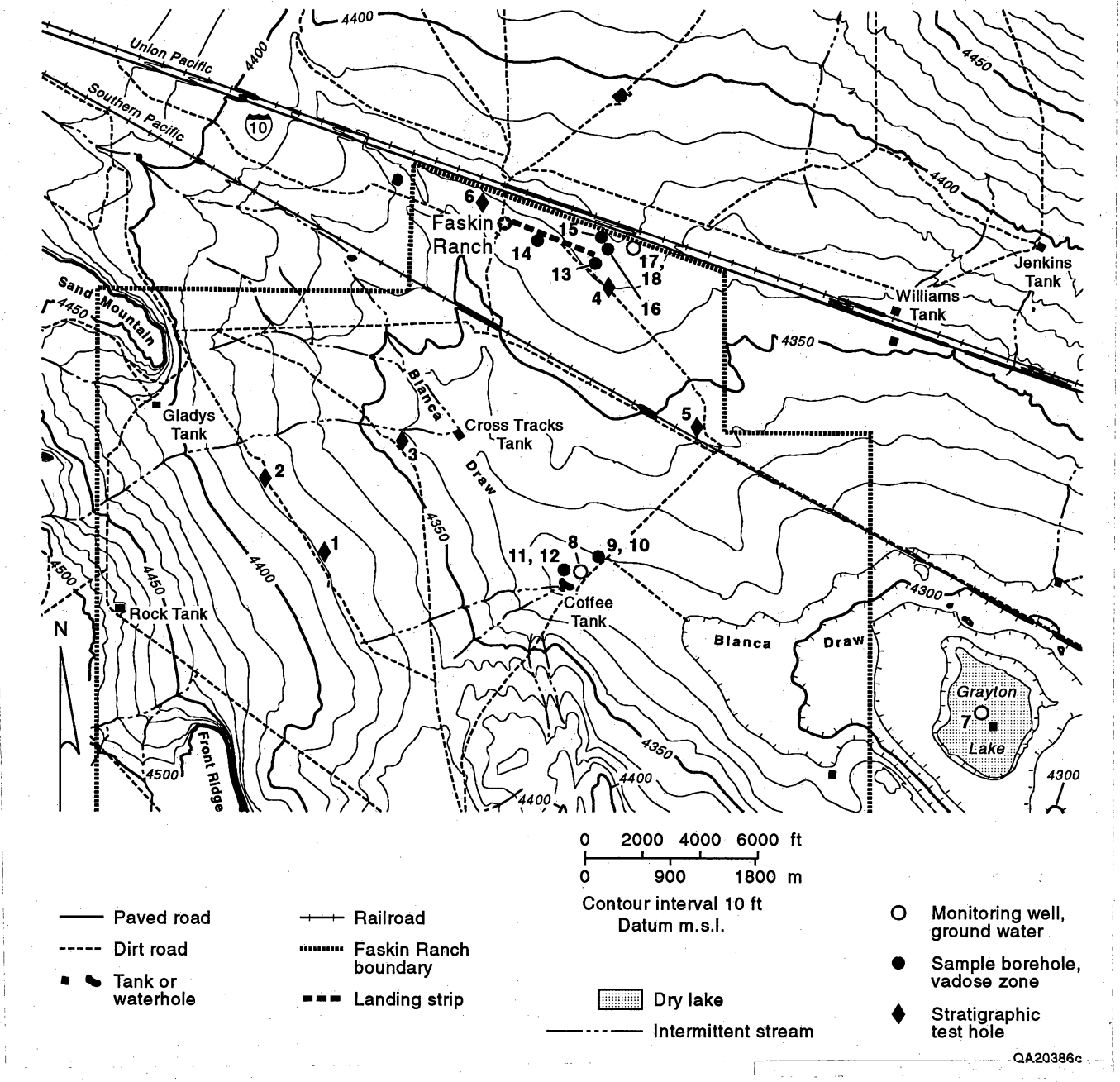

Figure 6. Map of northern Faskin Ranch area showing locations of boreholes. Boreholes drilled by the BEG are prefixed YM.

rocks are exposed elsewhere in the Sierra Blanca–Eagle Flat region and locally occur beneath the basin-fill sediments.

The upper basin-fill deposits in the vicinity of the proposed repository site are composed of poorly consolidated sand and silt, with lesser amounts of clay and gravel. Pedogenic structures are present throughout. Typical characteristics of the basin-fill sediments encountered in boreholes near the proposed site are shown in figure 7. Mineralogic composition of the fine-grained basin-fill deposits, as determined by X-ray and thin-section analysis, is quartz, feldspar, kaolinite, illite-smectite, calcite, and a trace of amphibole. Textural analyses currently available indicate 20 to 40 percent clay, 40 to 60 percent silt, and about 20 percent fine sand. Basal sediments deposited on or near the bedrock within the basin, or near the margins of the basin, are composed primarily of gravel.

Basin-fill sediments beneath Grayton Lake (fig. 6) were sampled in borehole YM-7. The uppermost 2 ft (0.6 m) in borehole YM-7 are silts. From 2 to 22 ft (0.6 to 6.7 m), the sediments are composed of clay and silt that are locally gleyed and are interpreted to represent deposition in a playa environment. Below the presumed Grayton Lake sediments are silts and fine sands similar to sediments in cores from boreholes at Faskin Ranch. Only a little gravel lies at the base of the basin-fill sediments in borehole YM-7. The underlying bedrock, the Cretaceous Cox Sandstone, was encountered at about 109 ft (33.2 m) below surface.

Fissurelike Features

Most of the basins in the Trans-Pecos region locally contain features characterized by generally linear patterns of holes, pipes, cracks, and/or collapse structures developed at the surface of the basin-fill sediments. Some of these features can be tentatively identified on aerial photographs by linear vegetation anomalies that are not apparently induced by human activities. Some of these surface features are demonstrably or presumably underlain by tensional fractures that extend to significant depths (several meters to a few tens of meters or

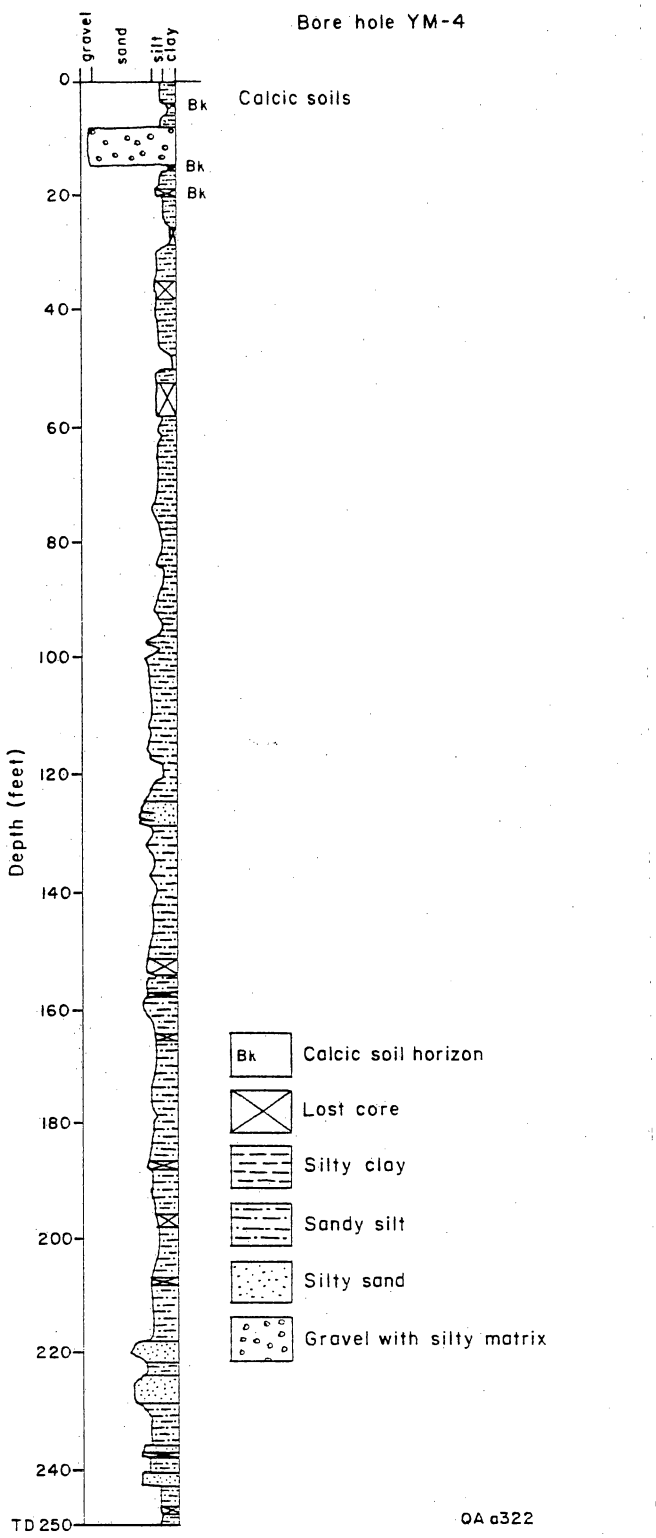

Figure 7. Lithologic log of borehole YM-4. Dominant grain size is very fine sand and silt, coarsening toward the base of the core. The upper 20 ft (6 m) of this borehole had poor recovery because the weakly consolidated nature of the sediments; lithology based on bagged samples. See figure 6 for the location of borehole YM-4.

more); such features, as for example those near Fort Hancock, Texas (Baumgardner and Scanlon, in press) and near Picacho, Arizona (for example, Jachens and Holzer, 1979), have been called "fissures." The possible modes of origin of fissurelike features include piping, desiccation, seismic activity, lowering of the water table, animal burrows, sediment compaction, or a combination of processes. The multiple potential modes of origin and the absence of a precise definition of a fissure have led us to use the term "fissurelike" to describe features found locally at the Faskin Ranch and in the surrounding area that share some characteristics with the "true" fissures described from other areas.

Fissurelike features are typically expressed at the Faskin Ranch as shallow, elongate trough-shaped features or as alignments of subcircular holes or depressions in the wash and interfluvial deposits. They have been identified in Blanca Draw and related tributaries (fig. 8) and outside the washes west of Blanca Draw. The highest concentration of fissurelike features found to date is in a tributary to Blanca Draw south of the Southern Pacific railroad tracks and north of Cross Tracks Tank (figs. 8 and 9). Other local concentrations of similar features occur upstream from Cross Tracks Tank and Coffee Tank and along Blanca Draw as it enters the Edwards Ranch to the east. Isolated fissurelike features are present in Blanca Draw upstream from Cross Tracks Tank and in a swale east of Blanca Draw.

Fissurelike features also occur elsewhere in the Sierra Blanca–Eagle Flat area outside of the Faskin Ranch. For example, on the Hoover property west of the northern Faskin Ranch, near Partition Tank east of Faskin Ranch, and in Eagle Flat Draw east-southeast of Grayton Lake. These fissurelike features are longer and generally better defined that those at Faskin Ranch. A 0.75-mi-long (1.2-km) linear feature marked by an increase in vegetation has also been identified on a sloping area adjacent to Blanca Draw northwest of Grayton Lake. Surface examination has revealed only a few shallow open voids or collapse features along the clearly discernible vegetation line. No fissurelike features have been identified on the proposed site for the repository (east of the road leading south from the Faskin ranch house and north of the Southern Pacific Railroad).

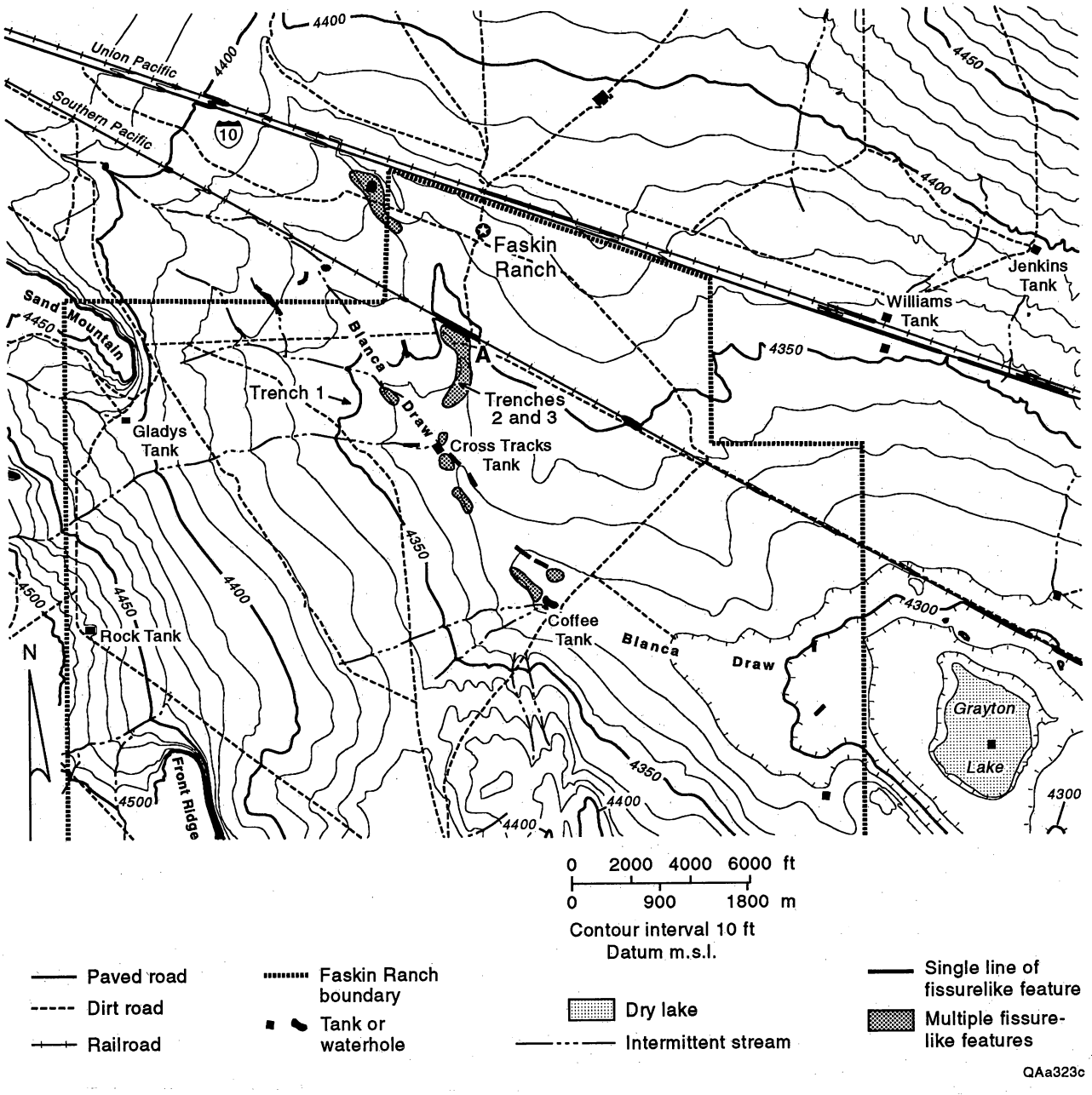

Figure 8. Preliminary map of occurrences of fissurelike features identified on Faskin Ranch. Detailed map of area A is shown in figure 9.

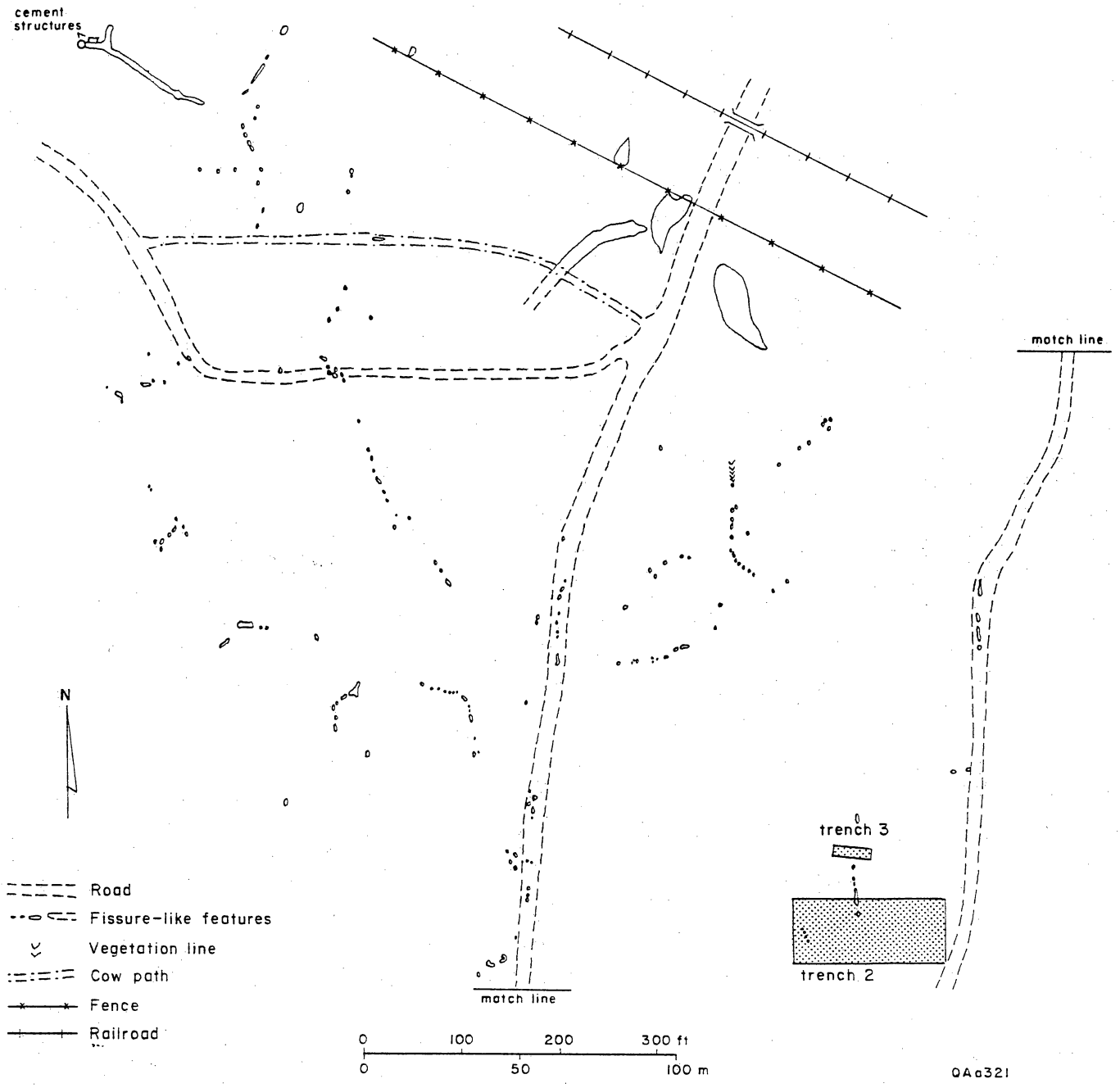

Figure 9. Map of fissurelike features in tributary to Blanca Draw, south of the Southern Pacific Railroad and north of Cross Tracks tank. Trenches 2 and 3 were excavated at the south end of the map area. Location of map area is shown on figure 8.

Fissurelike features on Faskin Ranch range in size from single holes, 4 inches (10 cm) or smaller in diameter and as much as 14 inches (35 cm) deep, to elongated depressions, tens of yards (meters) long and as much as 2 ft (70 cm) deep. These larger features are present immediately south of the Southern Pacific tracks at the eastern railroad bridge, north of Cross Tracks tank, and may have been modified by the activities of humans or of cattle. Most fissurelike features occur as linear arrays of open holes and shallow depressions. Typical single depressions range from 8 to 16 inches (20 to 40 cm) deep and are 1 to 6.6 ft (0.4 to 2 m) long.

The fissurelike features in the wash deposits are commonly associated with animal burrows or holes that may have originated as burrows. Animal burrows may be present because the wash deposits are relatively easy for the animals to excavate or because of the proximity to tanks or the presence of vegetation. Some burrowlike features exit from the bottom of the fissure walls, parallel with the floor, or they may enter from the middle of a fissure wall. Burrows may, in some cases, contribute significantly to the shape and orientation of the fissurelike features because they may focus water flow and initiate piping.

Three excavations were dug to evaluate the subsurface character of the fissurelike features and to compare the Faskin Ranch features to others described from elsewhere in the Trans Pecos (Baumgardner and Scanlon, in press). Trench 1 (fig. 8) was excavated across a line of relatively dense vegetation, which shows clearly on aerial photographs but is indistinct on the ground. The trench was dug to evaluate the subsurface expression of the linear vegetation anomaly. The excavation lies on a gentle slope several hundreds of meters from Blanca Draw in deposits tentatively identified as unit C because of the presence of a well-developed calcic soil. No subsurface cracks are obvious in the excavation below the organic-rich soil that is present on the projection of the vegetation linear. The near-surface calcic soil appears to be less well developed or is perhaps degraded where the vegetation linear projects across the excavation.

Trenches 2 and 3 were dug in wash deposits at the south end of an area with a relatively high concentration of fissurelike features (fig. 9). Neither of the trenches have subsurface fractures that are clay lined or sediment filled. A fracture is not evident beneath the voids and

collapse features (as was seen in the fissure excavations at Fort Hancock) that acts as a principle control on the location or the development of the fissurelike features. Minor unfilled cracks in the soils may be related either to pedogenic processes or to the physical disturbance caused by the excavation, but no evidence suggests that these have either influenced the formation of the fissurelike features or that they are present below the upper two meters of the excavation.

Lineaments

A lineament study of the Faskin Ranch and the surrounding Eagle Flat study area (figs. 1 and 2), as designated by the Texas Legislature, was completed this year. The results of that study are described in a contract report (Wermund, 1992), and the reader is referred to that report for a complete discussion of this topic.

The lineament study is based on an analysis of linear features that can be identified on stereographic pairs of aerial photographs of the study area. An effort was made to eliminate those linears due to human activities, such as fence lines and roads, so that only lineaments resulting from alignments of natural features are included in the analysis. The analysis includes an evaluation of the orientations, lengths, and densities of lineaments, and correlation, where possible, of lineament characteristics with the distribution of lithologies and terrain types in the study area.

Neotectonics

Investigations of the neotectonics of the site and surrounding region have included identifying and mapping faults that have had Quaternary (present to ~2 million years ago [mya]) movement and collecting geologic data to evaluate the seismic character of previous earthquakes. Our studies are based on aerial photograph interpretations and field work. Because the investigations are ongoing, the data presented in this report are preliminary. Additional details of the work in progress are reported in table 1 and in appendix I. Results of this study

Table 1. Characteristics of faults that offset Quaternary sediments

Location number	Basin	Fault	Maximum length (km)	Regional strike	Regional dip direction	Closest distance to Faskin Ranch reference point[1] (km)	Comments
	IN EAGLE FLAT STUDY AREA[2]						All faults primarily extensional.
1	Red Light Bolson	West Eagle Mountains–Red Hills fault	40	N35°–55°W	Southwest	10.5	Eighty percent of fault zone is inferred and covered; zone consists of at least three fault strands that have scarps that are 7, 1.5, and 1.2 km long; fault scarp closest to Faskin Ranch reference point is 13.5 km south-southwest of reference point and is 7 km long; fault zone length between most northwesterly and southeasterly scarps is 18 km, about half of inferred maximum length. West of Red Hills, middle Pleistocene deposits are offset between 1 and 2.5 m.
	WITHIN 50 KM OF EAGLE FLAT STUDY AREA[2]						
2	Hueco Bolson	Caballo fault	48	N20°–40°W	Southwest	23	Seventy percent of fault zone length is inferred and covered; zone consists of at least two fault strands; one strand is 11 km long and locally has a well-dissected subtle scarp; basin-fill deposits abut against bedrock along the surface trace of part of this fault; a second fault strand is expressed as a subtle, dissected scarp that is about 2.5 km long. Middle Pleistocene Madden gravel offset 24 m (estimate), late Pleistocene Ramey gravel offset 7 m, younger late Pleistocene Balluco gravel not faulted; offset of last surface rupture estimated to have been 1.7 m.

Table 1 (cont.)

Location number	Basin	Fault	Maximum length (km)	Regional strike	Regional dip direction	Closest distance to Faskin Ranch reference point[1] (km)	Comments
3	Red Light Bolson	West Indio Mountains fault	47	N30°–45°W	Southwest	34.5	Consists of several fault strands that have poor surface expression; more than 90 percent of zone is inferred or covered; one fault strand has good surface expression for 1.5 km and displaces middle Pleistocene deposits 1.8 to 2.5 m and probable upper Pleistocene deposits 0.9 m. Another fault strand displaces probable upper Pleistocene deposits 2.5 m. Landslide deposits on hanging-wall block.
4	Hueco Bolson	Ice Cream Cone fault	9	N15°–60°W	Southwest	29	Sixty percent of fault trace is covered and inferred; called fault 12 by Collins and Raney (1991a); upper Pleistocene Ramey gravel offset 13.8 m; younger late Pleistocene Balluco gravel not faulted.
5	Red Light Bolson	Nick Draw fault	2.5	N10°–15°E	West	29	About 1.2 km of fault is well-expressed scarp with Tertiary volcanic rocks faulted against Quaternary–Tertiary basin-fill deposits. Quaternary displacement uncertain.
6	Southeast Eagle Flat	East Eagle Mountains fault	5	N10°–20°W	East	32	Ninety percent of fault zone length is covered and inferred; only one short, 0.5-km fault scarp has good surface expression.

Table 1 (cont.)

Location number	Basin	Fault	Maximum length (km)	Regional strike	Regional dip direction	Closest distance to Faskin Ranch reference point[1] (km)	Comments
7	Wild Horse Flat	East Carrizo Mountain–Baylor Mountain fault	41	N10°–40°E	Southeast	37	Eighty-five percent of fault zone length is covered and inferred; three distinct scarps are 1, 1.2, and 3 km long; zone may be seismically segmented; scarps occur east and northeast of Carrizo Mountains; one strand displaces middle Pleistocene deposits 1.6 m; fault is covered east of Baylor Mountains.
8	Salt Basin	East Sierra Diablo fault	37	N10°W–N20°E	East	37	Sixty percent of fault zone length is covered and inferred; zone composed of a series of en echelon fault strands; at least 11 scarps exist along zone; two longest scarps are 5 and 2 km long. Upper Pleistocene–Holocene deposits are offset 1.5 m.
9	Southeast Eagle Flat	West Van Horn Mountains fault	27	N30°W–N15°E	West	38.5	Seventy percent of fault zone length is inferred and covered; northern part consists of 7-km-long eroded scarp at base of Van Horn Mountains and an en echelon 1-km-long eroded scarp at southwestern flank of Carrizo Mountains; southern part of fault zone is covered and inferred along western flank of Van Horn Mountains. Quaternary offset uncertain.
10	Hueco Bolson	Arroyo Diablo fault	15	N30°–60°W	Southwest	39	Ninety percent of fault trace is covered or inferred; called fault 10 by Collins and Raney (1991a); middle Pleistocene Madden gravel offset 1.6 to 3 m; late Pleistocene deposits not faulted; offset during last surface rupture was 0.6 m.

Table 1 (cont.)

Location number	Basin	Fault	Maximum length (km)	Regional strike	Regional dip direction	Closest distance to Faskin Ranch reference point[1] (km)	Comments
11	Hueco Bolson	Amargosa fault	70	N40°–50°W	Northeast	41	Strike-slip component suggested by Barnes and others (1989), although in areas studied by Collins and Raney (1991a) normal slip is dominant; fault zone is well expressed at surface along most of its length; middle Pleistocene deposits offset 23.5 m, older late Pleistocene deposits offset 6.5 m, and younger late Pleistocene deposits offset 2.5 to 4.5 m. Holocene deposits probably faulted on the basis of interpretations of aerial photographs; offset during last surface rupture was 1.6 to 2.5 m.
12	Hueco Bolson	Campo Grande fault	45	N40°–70°W	Southwest	42	Composed of three en echelon geometrical segments that are 21, 21, and 34 km long; middle Pleistocene deposits offset 10 m, older late Pleistocene deposits offset 3 m, and younger late Pleistocene deposits (estimated to be 25,000 to 100,000 years old) are not faulted; offset of last surface rupture was 1 to 1.5 m. Zone has been described in detail by Collins and Raney (1990; 1991a).
13	Lobo Valley	Fay fault	4	N5°–20°W	East	43	Consists of at least two en echelon fault scarps; 60 percent of fault zone length is covered and inferred. Middle Pleistocene deposits are offset 1.2 m.
14	Hueco Bolson	Arroyo Macho fault	1.5	N30°–40°E	Southeast	44	Middle Pleistocene deposits offset 2 m; called fault 11 by Collins and Raney (1991a).

Table 1 (cont.)

Location number	Basin	Fault	Maximum length (km)	Regional strike	Regional dip direction	Closest distance to Faskin Ranch reference point[1] (km)	Comments
15	Not within a basin	Deep Well fault	1.3	N10°–30°W	West	47	Located in north-central part of Van Horn Mountains; scarp is at contact between Quaternary(?) deposits and older bedrock. Quaternary offset uncertain.
16	Lobo Valley	East Van Horn Mountains–Sierra Vieja fault zone	61	see below	see below	48	Normal dip-slip and strike-slip components have been considered (Sanford and Toppozada, 1974; Dumas and others, 1980; Doser, 1987); zone consists of a series of en echelon fault strands; three geometrical segments exist; unknown if fault zone is seismically segmented; 85 percent of the fault zone is well expressed at the surface by fault scarps. Sierra Vieja segment has been interpreted as the active fault of the 1931 Valentine earthquake, MM intensity VII and M = 6.4 (Doser, 1987). Neal fault displaces middle Pleistocene deposits at least 5 m. Mayfield fault displaces middle Pleistocene deposits as much as 6 m. Sierra Vieja fault displaces possible middle Pleistocene deposits as much as 8.2 m and possible upper Pleistocene–Holocene deposits 3.5 m.
		includes three segments:					
		a. Neal fault	18	N10°W–N25°E	East	48	
		b. Mayfield fault	20	N30°–55°W	Northeast	57	
		c. Sierra Vieja fault	25	N30°W–N20°E	East	77	
17	Lobo Valley	West Wylie Mountains fault	20	N10°–30°W	Southwest	48	Eighty-five percent of fault zone length is covered and inferred; two scarps about 1 km long exist in Quaternary(?) surficial deposits, and the fault has been mapped in bedrock in two areas.

Table 1 (cont.)

Location number	Basin	Fault	Maximum length (km)	Regional strike	Regional dip direction	Closest distance to Faskin Ranch reference point[1] (km)	Comments
18	Green River Basin	Indio fault	6	N20°–45°W	Southwest	50	Probably recurring Tertiary–Quaternary(?) extensional movement on preexisting fault; about 6 km (length) appears to have had Tertiary movement; Quaternary displacement uncertain; total fault length is 20 km.
19	Green River Basin	China Canyon fault	1.5	N10°–20°W	East	52	Quaternary offset uncertain; subtle scarp about 1 km long.
20	Green River Basin	Green River fault	9	N15°–30°W	Southwest	52	Quaternary offset uncertain; three subtle scarps between 1.5 and 2 km long.
21	Salt Basin	East Flat Top Mountains fault	23	N25°W–N5°E	East	53	Series of en echelon faults; scarps between 0.5 and 2 km long; 80 percent of zone is covered and inferred.
22	Salt Basin	North Sierra Diablo fault	13.5	N75°–85°W	North	54	Seventy percent of zone is covered or inferred; 4-km-long scarp.
23	Llanos de Chilicote	Sierra de la Lagrina fault	41	N5°–35°W	West	61	Tertiary–Quaternary(?) offset inferred from San Antonio El Bravo sheet (Coordinación General de los Servicios Nacionales de Estadistica, 1982). Surface expression of fault and Quaternary offset is uncertain on basis of Gries (1979; 1980) hypothesis that Cenozoic extension in this area may have reactivated older structures and caused flowage of thick evaporite sequences and may not be expressed as faults at the surface.

Table 1 (cont.)

Location number	Basin	Fault	Maximum length (km)	Regional strike	Regional dip direction	Closest distance to Faskin Ranch reference point[1] (km)	Comments
24	Salt Basin	West Delaware Mountains fault	64	N25°–45°W	Southwest	64	Broad zone consisting of series of numerous fault strands; most scarps are between 1 and 7 km long.
25	Llanos de Chilicote	Sierra Labra fault	22	N0°–30°W	West	65	Tertiary–Quaternary(?) offset inferred from San Antonio El Bravo sheet (Coordinación General de los Servicios Nacionales de Estadistica, 1982). Surface expression of fault and Quaternary offset is uncertain on basis of Gries (1979; 1980) hypothesis that Cenozoic extension in this area may have reactivated older structures and caused flowage of thick evaporite sequences and may not be expressed as faults at the surface.
26	Hueco Bolson	Acala fault	10	N40°–50°W	Southwest	68	Composed of two scarps (faults 7 and 8 of Collins and Raney [1991a]); scarps offset middle Pleistocene deposits 18 and 4 m.

[1] Faskin Ranch reference point = latitude: 105°15', longitude: 31°07'30"
[2] Study area designated by Texas Legislature

will be used by other contractors to evaluate seismic risk to the repository and for repository design.

The study area includes the Eagle Flat area, as designated by the Texas legislature, and the adjacent region out to 31 mi (50 km) from the boundary of the Eagle Flat area (fig. 10). The study region contains intermontane basins and associated normal faults that formed in response to Basin and Range extensional tectonism that began about 24 Ma ago. This extensional tectonism continues to the present and is responsible for ongoing seismic activity and historic earthquakes such as the 1931 Valentine event.

Table 1, read in conjunction with figure 10, provides a good summary of our progress. Identified faults are related to their associated basin, and the inferred maximum cumulative length of the fault strands and the regional strike and dip of the faults are recorded. The closest distance of each fault to an arbitrary reference point at Faskin Ranch (latitude 105°15', longitude 31°07'30") and comments on the characteristics of each fault are also noted.

This study has not identified any Quaternary fault scarps in the Blanca Draw portion of the Eagle Flat area. The closest Quaternary fault scarp to the proposed site at Faskin Ranch is about 4.3 mi (7 km) long and occurs in Red Light Draw 8.4 mi (13.5) km south-southwest of the Faskin Ranch reference point. Buried or inferred extensions of the fault strands may occur as close as 6 mi (10 km) to the reference point. Middle Pleistocene age deposits, probably 250,000 to 500,000 yr old in this area, are offset between 3.3 and 8.2 ft (1 and 2.5 m).

Natural Resources

The location of mineral and geothermal resources within the 400-mi^2 (1,036-km^2) Eagle Flat study area (Allamoore, Grayton Lake, Devil Ridge, Sierra Blanca, Bean Hill, and Dome Peak 7.5-minute topographic quadrangles; figs. 1 and 11) were described as part of the geologic characterization program. To more fully describe the regional trends and mineralogic associations, mineral localities were also characterized within a larger 900-mi^2 (2,304-km^2)

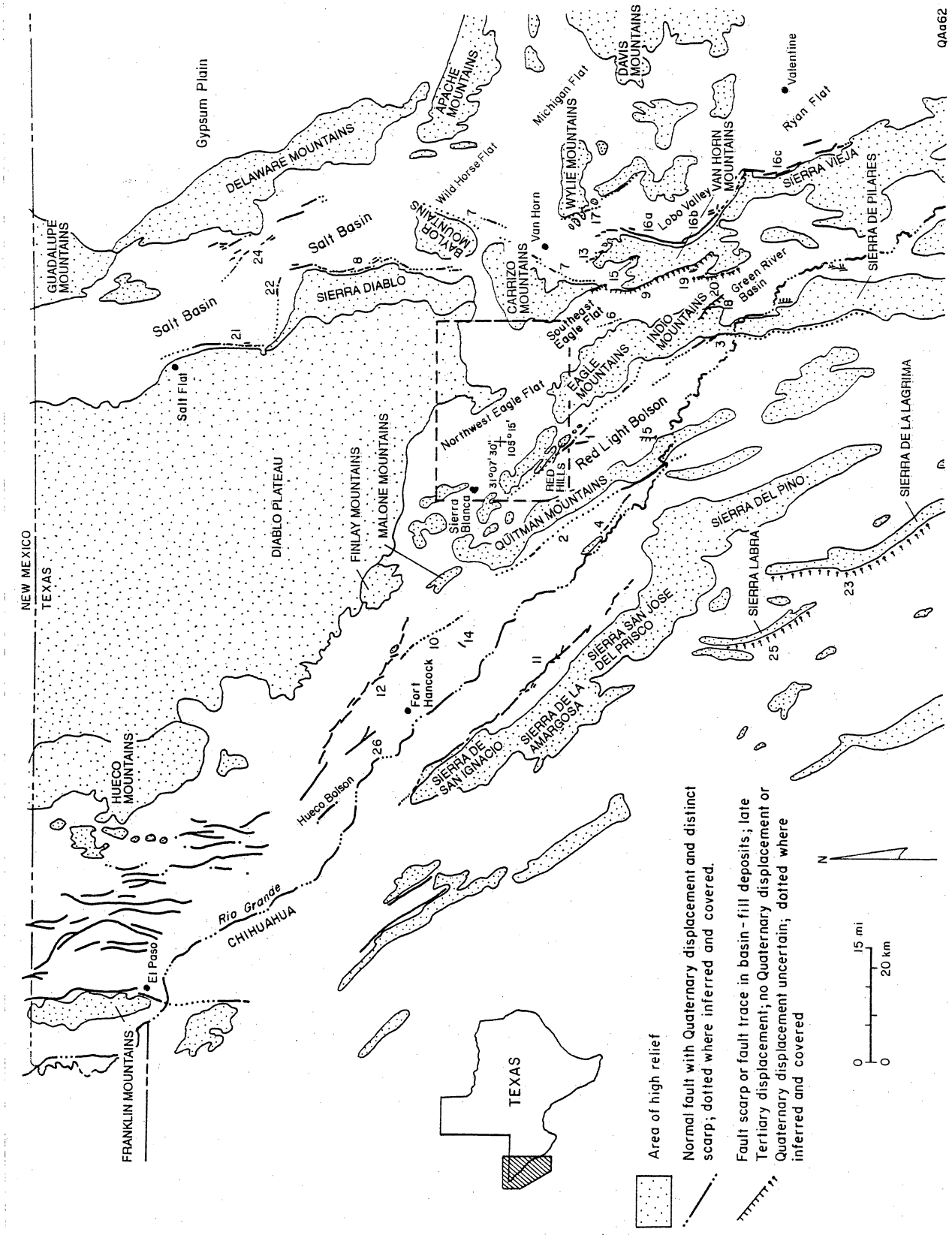

Figure 10. Map of faults that are known to have had or may have had offset during the late Tertiary or Quaternary. Map includes faults with definite surface manifestations (scarps) and inferred extensions.

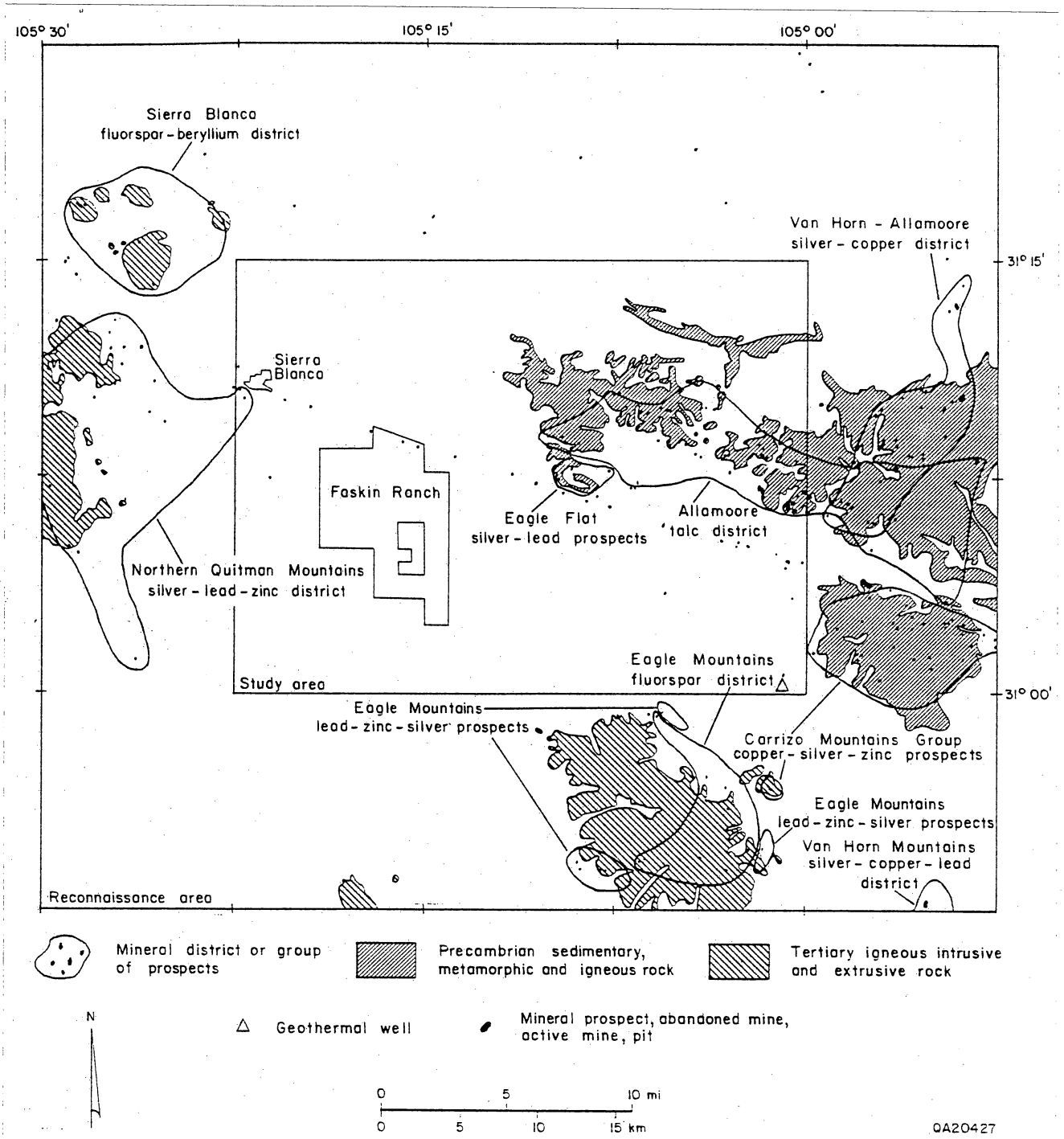

Figure 11. Map of Eagle Flat study area and surrounding reconnaissance area showing locations of mineral prospects and districts.

reconnaissance area that includes 16 adjacent 7.5-minute quadrangles (fig. 11). A complete description of this work is being prepared as a topical contract report (Seni, 1992).

This compilation (see appendix II) includes active mines, abandoned mines, prospects, and quarries whose locations were determined by literature survey. Price and others (1983) compiled mineral localities and organized them into districts that are characterized by a common mineralogic association, host rock, or mode of origin. Their compilation includes locality name, location by latitude/longitude, status of mining operation, commodity, and mineral district and is the primary basis for locality information. Additional localities were obtained from the BEG Mineral Producers Index, the Railroad Commission of Texas (Mined Lands Inventory), and U.S. Geological Survey 7.5-minute quadrangle maps. Detailed geologic data from historic mines and mineral occurrences are also available in a wide variety of referenced material.

A unique identification number is assigned to each locality on the basis of its location on a 7.5-minute topographic map (Texas numbering system) (fig. 12). No information was gathered on hydrocarbon or water resources as part of this study. Geothermal resources are indicated by hot springs and water wells that produce anomalously hot water. Although uranium prospects and radioactive anomalies are reported in the region, no commercial deposits have been identified and no significant anomalies (<100 ppm) occur within the study area or larger reconnaissance area. Anomalous (50 to 80 ppm) uranium concentrations are associated with beryllium-fluorspar in the Sierra Blanca peaks.

Mining districts and prospects are outlined in figure 11. Current mineral production in both the study area and the larger reconnaissance area is limited to talc from the Allamoore talc district and aggregate (sand and gravel or crushed stone). Most of the mineral localities are prospects that never had mineral production or were mines active before the early 1900's through the 1940's. Although many prospects for base and precious metals exist, no precious metals mining is currently active, and only a very small volume of precious metal ore is known to have been shipped from the study area. During the 1970's and early 1980's, a dramatic rise

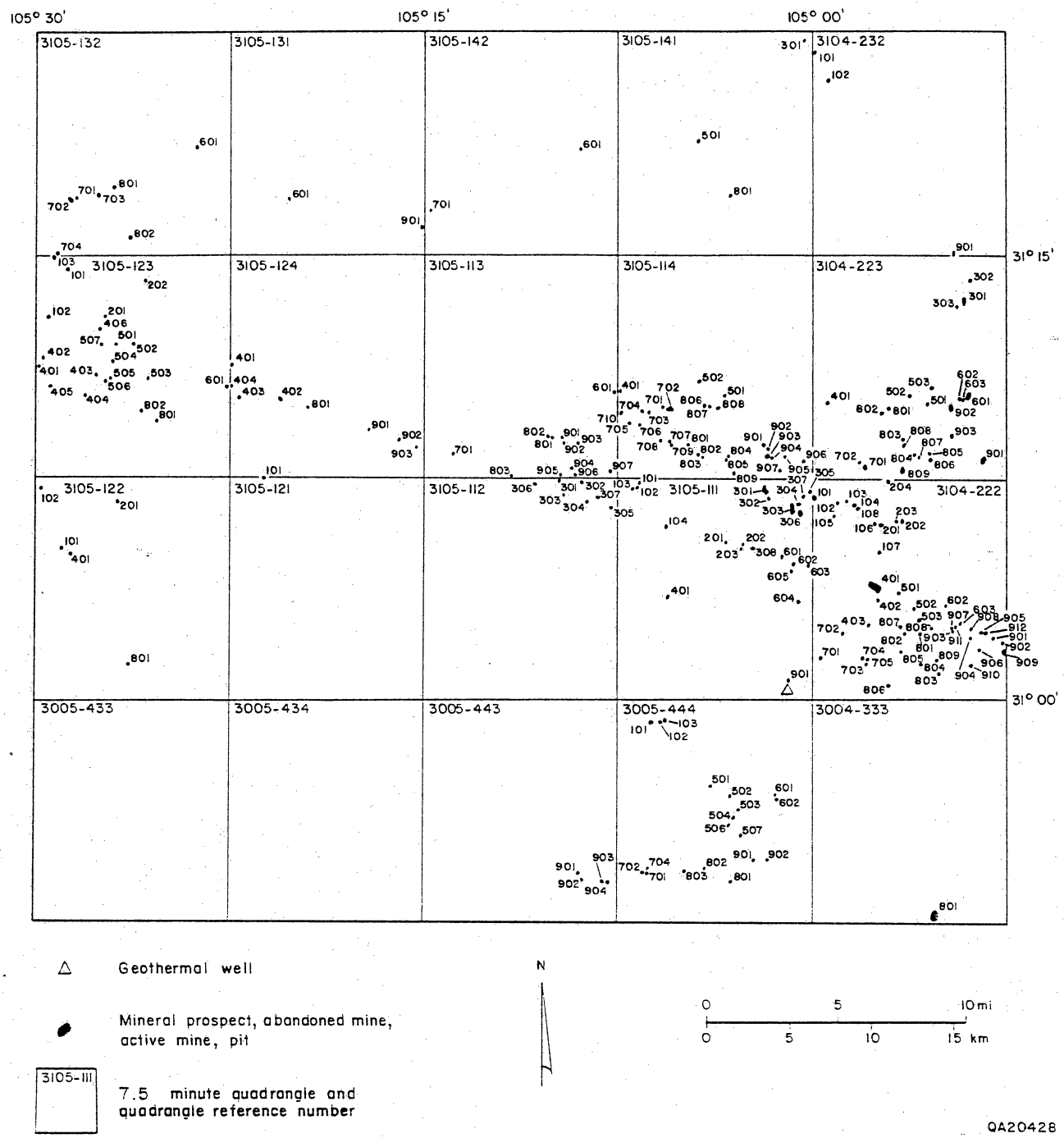

Figure 12. Map of Eagle Flat study area and surrounding reconnaissance area showing unique numbers assigned to mineral prospects and mines. Refer to appendix II for compilation of mineral inventory data.

in prices of precious metals supported a brief flurry of exploration, but no new production resulted from this activity.

In the surrounding reconnaissance area, precious and base metal mining has occurred in the past, but mining efforts are currently inactive. Historic production was dominated by (1) the Van Horn–Allamoore silver and copper district (Hazel, Blackshaft, and Sancho Panza mines) and (2) the Eagle Mountains fluorspar district (Spar Valley area and Eagle Spring mines). Subordinate precious and base metals production came from (1) the Northern Quitman Mountains (Bonanza mine) and (2) the Van Horn Mountains (Plata Verde mine). Beryllium-bearing fluorspar deposits were identified in the early 1970's in association with intrusions in the Sierra Blanca and Round Top Mountains area. The Sierra Blanca fluorspar- beryllium district probably hosts large mineable reserves, but these are not being produced.

The age, rock type, and tectonic history of the outcropping strata largely control the distribution of mineral resources. Talc and other industrial minerals are associated with the metamorphosed phyllites of the Allamoore Formation. Hydrothermal activity associated with Tertiary intrusions introduced metal-rich (Ag, Cu, Pb, Zn) and fluorine-rich (fluorspar) fluids, which reacted with nearby country rock and yielded veins and replacement bodies. Such veins and replacements occur in topographic highlands associated with the Eagle Mountains, Carrizo Mountains, Van Horn Mountains, and Quitman Mountains. Price and others (1985) related silver-copper ores that occur in veins and strata-bound deposits in Precambrian, Permian, and Cretaceous sandstones (Van Horn–Allamoore silver and copper and Van Horn Mountains silver, copper, lead districts) to low-temperature, strata-bound red-bed copper deposits. Sand and gravel deposits are typical Cenozoic bolson-fill sediments associated with late Cenozoic basins.

HYDROGEOLOGIC INVESTIGATIONS

Hydrogeologic investigations are an essential component of the characterization of the proposed site. Understanding the occurrence and movement of water, both in the vadose

("unsaturated") zone and in the saturated zone, forms the basis for performance assessment analyses and for the design and licensing of the proposed facility. Through these investigations we will characterize hydrogeologic processes at the site and in the surrounding region, and we will attempt to describe how the hydrogeologic systems have changed over time.

Many of the previously described geologic studies, as well as the geophysical investigations to be described in a following section, will provide information needed to construct the geologic framework for hydrogeologic models. Hydraulic and chemical attributes of the system are being measured at the Eagle Flat site and from the adjacent region. Hydraulic attributes include soil moisture content, soil water potential, hydraulic conductivity, and hydraulic head. Chemical attributes include measurement of stable and radioactive isotopes in the vadose and saturated zones and composition of major ions in the saturated zone. Analysis of hydraulic and chemical parameters will provide data to evaluate the direction and rate of water movement. Where appropriate, data from previous studies at the Fort Hancock site will be used to supplement the data base developed for the Eagle Flat site. Numerical models will be used to evaluate controls of various hydrologic and hydrochemical processes.

Vadose Zone Studies

The vadose zone is that part of the hydrogeologic environment that lies between the surface and the top of the saturated zone (the top of the "water table") at depth, the soils, sediments, and rocks of the vadose zone being generally unsaturated. Our vadose zone studies are restricted to the Eagle Flat study area. Near the site at Faskin Ranch, the vadose zone is about 650 to 800 ft (200 to 245 m) thick, and the proposed repository would be constructed in the shallow part of the zone. Data on the direction and rate of water movement in the vadose zone are important for performance assessment and facility design because such information can affect the fate of potential contaminants from the proposed repository.

Vadose zone hydrologic studies are being done only at the Faskin Ranch. The objective is to evaluate moisture flux in the shallow unsaturated zone at the proposed site (table 2) using hydraulic and chemical approaches. Hydraulic data include moisture content and water potential. Water-potential data can be used to assess the direction of water movement because water flows from regions of high to low water potential. The chemical approach involves using chloride mass balance methods to estimate moisture fluxes in the vadose zone. High chloride concentrations indicate low moisture flux because chloride is concentrated by evapotranspiration whereas low chloride concentrations indicate higher moisture flux because chloride is leached from the soil.

The first phase of the study at Faskin Ranch focused on collecting soil samples for laboratory analysis of grain-size distribution, moisture content, water potential, and chloride concentration. Soil samples were collected from eight boreholes (YM-9 to YM-16) that ranged in depth from 18 to 54 ft (5.6 to 16.6 m) (table 1; fig. 6). The number of samples from each borehole ranged from 16 to 36, with smaller sampling intervals (0.3 to 1.0 ft [0.1 to 0.3 m]) occurring close to land surface—approximately the upper 16 ft (5 m), where hydraulic and chemical parameters are most variable and larger sampling intervals (generally 2.6 ft [0.8 m] or more) occurring at depth. The boreholes (fig. 6) sampled different geomorphic settings: (1) ephemeral stream (Blanca Draw; boreholes YM-11 and YM-12) setting, (2) the interstream (boreholes YM-9, YM-10, YM-13, YM-14) setting, and (3) in and adjacent to a borrow pit (YM-15, YM-16). The interstream boreholes are located in sandy (borehole YM-13) and silty (borehole YM-14) surface soils (E1 and E2 deposits). Water potentials are measured using the Decagon psychrometer SC-10 sample changer and a newly acquired water activity meter (Model CX-1), both manufactured by Decagon Devices, Pullman, WA. Procedures for field sample collection and laboratory analyses can be found in Scanlon and others (1991) and in Scanlon (1992).

Laboratory analyses of moisture content, water potential, and chloride concentration are in progress. Figure 13 is an example of the variations in gravimetric moisture content, water

Table 2. Tabulation of boreholes drilled for vadose zone sampling showing status of analytical work and geomorphic setting of borehole. Samples to be analyzed for water potential (WP), chloride (Cl), and moisture content (MC). Location of boreholes shown on figure 6.

Hole ID	Depth (m)	No. of samples (*)	Completed analyses (*)	Geomorphic setting
YM-9	14.6	36	WP, Cl, MC	Interstream, just outside flood plain
YM-10	10.3	33	Cl, MC	do
YM-11	9.3	20	MC	Blanca Draw, upper flood plain
YM-12	5.6	16	WP, MC	do
YM-13	11.3	26	WP, MC	Interstream, sandy surface material
YM-14	9.6	22	MC	Interstream, silty surface material
YM-15	16.6	33	MC	Borrow pit
YM-16	14.5	29		Adjacent to borrow pit

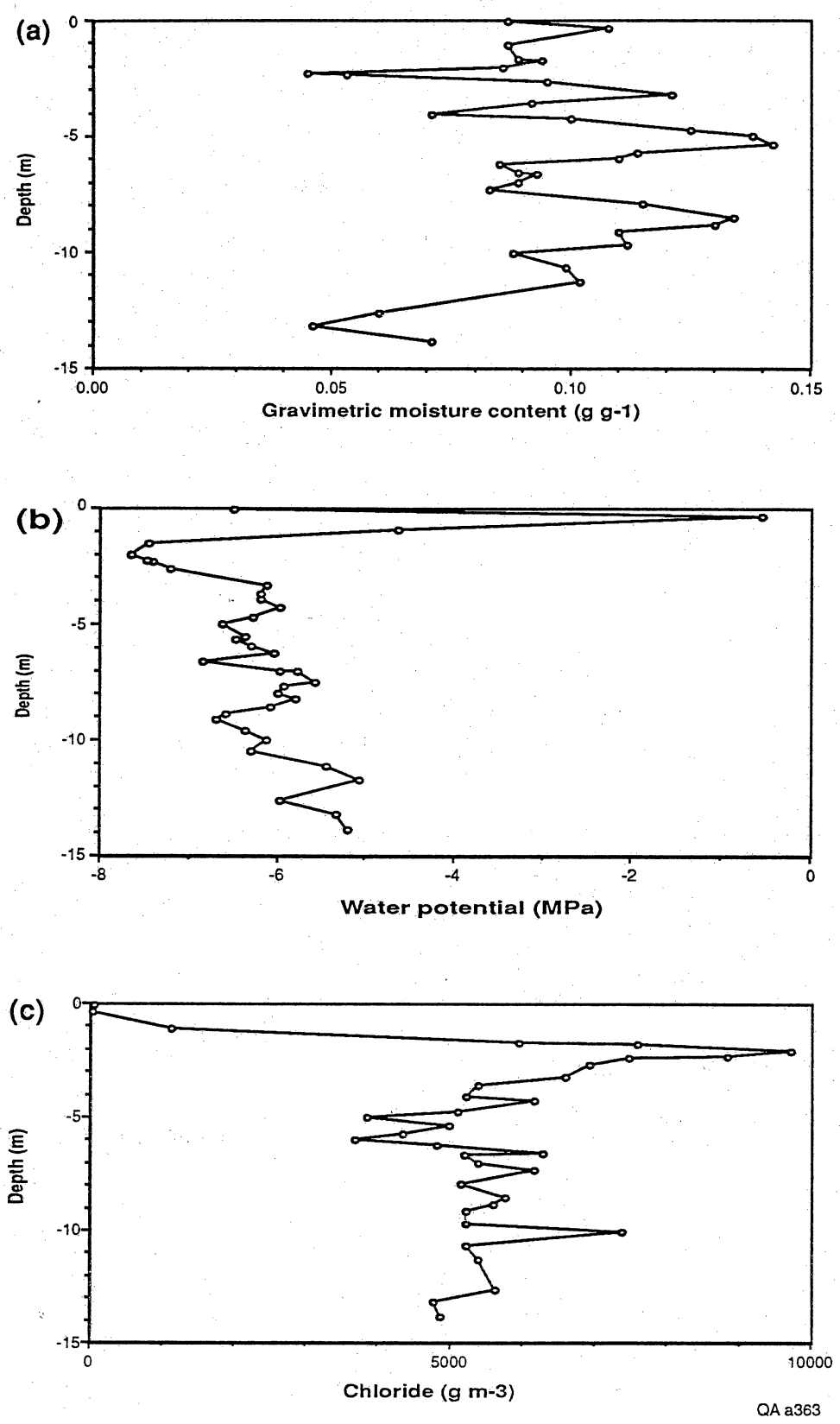

Figure 13. Variations in (a) gravimetric moisture content, (b) water potential, and (c) chloride in soil samples from borehole YM-9. For location of borehole, see figure 6.

potential, and chloride in soil samples from a borehole, YM-9, at Faskin ranch. These data are being used in numerical modeling studies to evaluate controls on subsurface flow.

Saturated Zone Studies

Saturated zone studies are being conducted on two scales: at a local scale on the Faskin Ranch in the Eagle Flat study area (fig. 1) and on a regional scale (fig. 14). The regional studies extend from the upper reaches of Blanca Draw in the north, to the Rio Grande to the south. The east edge is delimited by the western Carrizo and Van Horn Mountains (Eagle Flat Draw–Green River Valley), and by the east flanks of the Quitman Mountains (Red Light Draw).

Hydrochemical sampling has been conducted jointly at five wells by scientists from The University of Texas at El Paso (UTEP) and BEG. Because processes (such as mixing in the well bore or reactions between the ground water and the well casing) may alter water chemistry, special care has been taken to collect samples only after sufficient water has been produced such that the eH of the water has stabilized. Stable Eh values are probably good indicators of stable concentrations of chemical constituents. The UTEP scientists are attempting to test the validity of this assumption by quantifying the relationship between changes in Eh and water chemistry. Seventy-one samples were collected but results are not yet available.

Monitor Wells

Three monitor wells, YM-7, YM-8, and YM-18 (fig. 6), have been drilled as part of this project. One well, YM-7, was constructed off-site at Grayton Lake; two wells, an up-gradient and a down-gradient well (YM-18 and YM-8, respectively), are site-specific monitor wells; drilling of a third down-gradient, site-specific monitor well (YM-19), began in August 1992. Those parts of wells YM-8 and YM-18 that encountered basin-fill sediments have been geophysically logged. Pumping tests will be run, and quarterly sampling will be started once well YM-19 is complete.

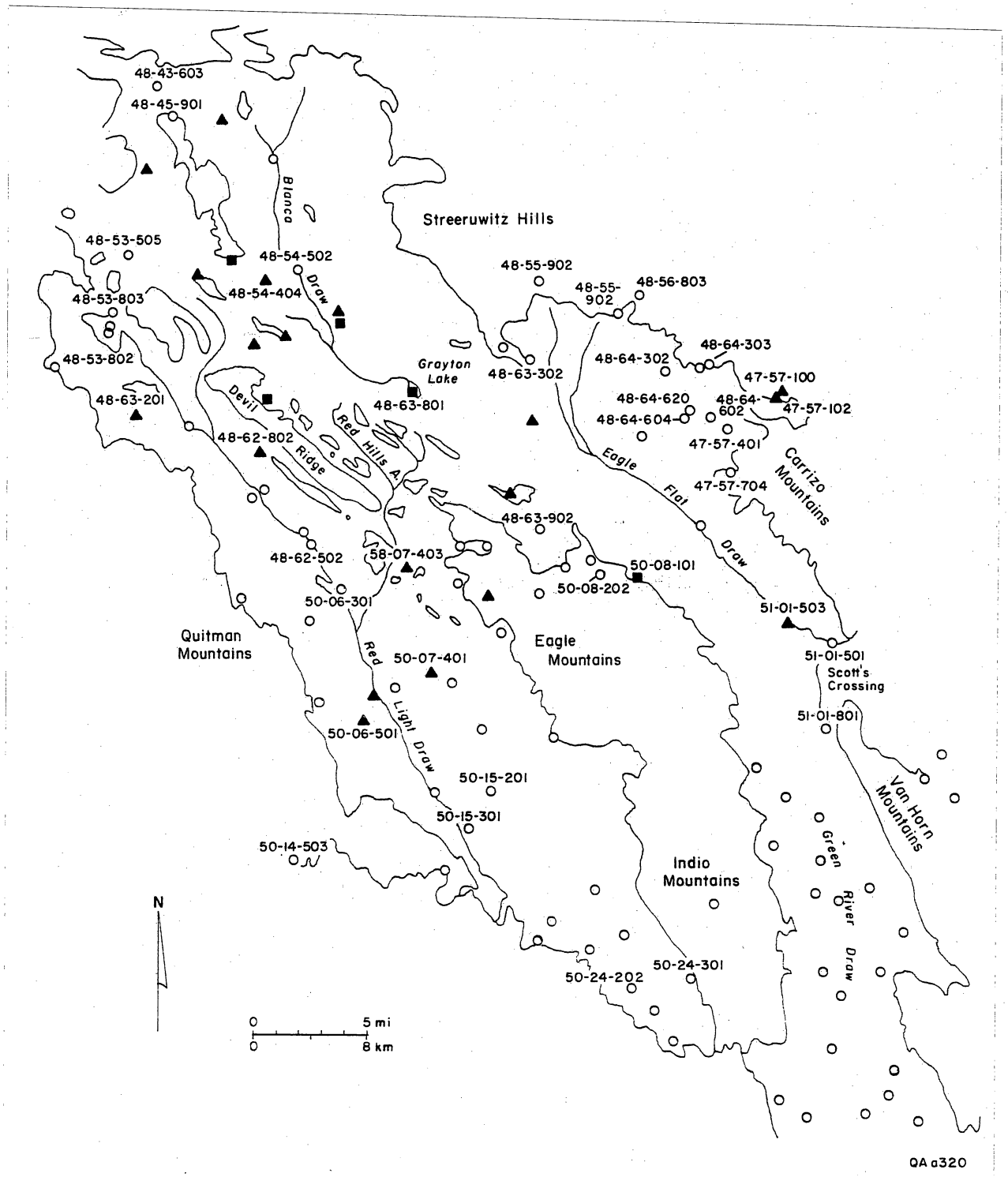

Figure 14. Location map of wells that will be used to construct the regional potentiometric map. Wells for which the depth is listed as reported or estimated by the Texas Water Development Board are marked by triangles. Wells for which the depth to water was measured by the Texas Water Development Board are marked by darkened circles. Locations of wells where water levels were recorded by BEG are indicated by darkened squares. Wells with identification numbers are those sampled for hydrochemical analysis.

Pumping tests were performed at the Grayton Lake monitor well (YM-7). This well is completed in Cretaceous limestone at a total depth of 882 ft (269 m), with a 160-ft (49-m) screened section from 715 to 875 ft (218 to 267 m). Water level determined before the pumping tests was at 654.5 ft (199.5 m) below surface; the water column in the borehole was 228 ft (69.5 m) thick. Pumping tests were performed over pumping periods of 7, 19, and 64.5 hours at rates of 6 to 50 gal/min (22.7 to 189.3 L/min). Plots of the recovery and drawdown data from the long-term pumping test are most comparable to idealized curves for leaky confined aquifers. Averaged over the entire water column, transmissivity values are 40.3 ft^2/day (3.74 m^2/day) (recovery phase) to 79.8 ft^2/day (7.4 m^2/day) (drawdown phase); permeability values are 0.18 ft/day (0.055 m/day) (recovery phase) to 0.35 ft/day (0.11 m/day) (drawdown phase). Transmissivity and permeability values determined using the Theis recovery method were 81.0 ft^2/day (7.5 m^2/day) and 0.35 ft/day (0.11 m/day), respectively.

Potentiometric Surface

Data on the elevation of the top of the static water level from approximately 100 wells (fig. 14) have been compiled to define a preliminary version of the regional potentiometric surface. This map will integrate data from existing wells on a regional scale, data from three wells completed by the BEG (one additional well is in progress) at the Faskin Ranch, and data reported by the Texas Water Development Board (TWDB). The TWDB data will be used for those wells where static water levels can no longer be measured. The recent measurements made by the BEG help to verify the older TWDB data and add additional data points to refine the potentiometric surface.

Preliminary data on the potentiometric surface suggest that ground water is shallowest and is being recharged in topographically high areas (Eagle Mountains, Streeruwitz Hills, Carrizo Mountains, Quitman Mountains), and flows toward the basinal areas.

Regional Hydrochemistry

The regional hydrochemistry study includes collection of water samples for analysis of major ions, trace elements, stable isotopes ($\delta^{18}O$, $\delta^{2}H$, and $\delta^{13}C$), and radioactive isotopes (^{3}H and ^{14}C). The resulting data base will to be used to identify recharge and discharge areas, to estimate ground-water ages and regional flow rates, and to construct a quantitative model of the hydrochemical evolution of the ground water.

Fifty-two samples have been collected from wells in the region (fig. 14). The BEG Mineral Studies Laboratory (MSL) has completed analyses of major ions and stable isotopes in 29 samples. The remaining 23 samples should be analyzed within the next few weeks. Analysis of radioactive isotopes are being conducted by laboratories at the University of Arizona (^{14}C) and the University of Miami (^{3}H). Samples will be collected from additional wells drilled in conjunction with this project, but almost all of the regional sampling has been completed. Analyses published by the Texas Water Development Board will be used to supplement the data base. Table 3 lists the disposition of the samples collected for this study, and table 4 lists the results of the completed analyses.

The preliminary results of the available analyses suggest that there are marked differences exist in the hydrochemical and isotopic characteristics of ground water across the area. Ground water in Blanca Draw (fig. 14) is dominated by sodium-sulfate-chloride ions, and total dissolved solids are as much as 3,000 mg/L Uncorrected carbon-14 values are 8 to 12 percent modern carbon, suggesting relatively old radiometric ages. Tritium activities indicate that no direct evidence exists of post-1951 recharge.

Ground water in Eagle Flat and Green River Valley ranges from calcium-bicarbonate and sodium-bicarbonate to sodium-magnesium-calcium-bicarbonate-chloride. Total dissolved solids are typically less than 1,000 mg/L. Carbon-14 and tritium values suggest that active recharge may be occurring in the northeast parts of the Eagle Flat study area. Other isotopic data suggest that ground water in eastern Eagle Flat, south of the Carrizo Mountains, may be quite old. These

Table 3. Disposition of samples submitted for analysis.

	Ions*	$\delta^{18}O$*	$\delta^{2}H$*	$\delta^{13}C$-^{14}C#	^{3}H†	$\delta^{34}S$#
Analyzed	29	21	0	17	24	0
At Lab	23	23	44	19	17	11
Total	52	44	44	36	41	11

*Analysis by Mineral Studies Lab, Bureau of Economic Geology, The University of Texas at Austin
#Analysis by Laboratory of Isotope Geochemistry, University of Arizona
†Analysis by Tritium Laboratory, University of Miami

Table 4. Available analytical results of water well samples.

Sample	Owner	Well Name	Date	MG/L												Temp.	H3	C13	C14	Uncorrected C14 Age
ID Number	or Operator	or Location	Reported	Na	K	Mg	Ca	B	Cl	F	Br	NO3	SO4	HCO3	pH	Deg. C	TU	PDB	PMC	Years BP
48-56-803	Aguirre, C.	House	3/30/92	62.90	<1.54	30.00	55.40	0.17	39.00	0.40	<0.01	27.00	78.50	287.00	7.30	19.20	3.67	-6.6	62.8	3846
51-10-111	Alford, L.		1/22/92	104.00	2.04	5.46	29.90	0.22	28.50	1.94	<0.01	9.65	75.90	254.00	7.61	20.80				
51-01-501	Alford, L.	Lado	3/30/92	132.00	<1.54	1.13	7.83	0.41	8.30	3.93	<0.01	4.26	43.30	279.00	8.12	14.00	0.14	-6.9	6.8	22223
51-01-501	Alford, L.	Lado	8/12/92	134.00		1.17	8.41	0.39	8.76	3.63	<0.25	3.98	43.70	283.00	8.02	24.50				
47-57-401	Ashley, J.		1/22/92	284.00	5.58	65.30	47.60	1.34	107.00	5.77	<0.01	14.90	449.00	494.00	7.48	18.80	2.22			
48-64-604	Booth, M.	House	1/22/92	115.00	2.24	37.40	45.90	0.56	54.00	1.84	<0.01	17.00	175.00	315.00	7.40	20.50	3.02	-6.3	45.1	6583
48-63-302	Booth, M.	Winters	1/22/92	148.00	2.85	40.90	43.00	0.37	62.00	2.44	<0.01	8.70	197.00	354.00	7.56	23.10	0.37	-7.9	27.6	10642
48-63-302	Booth, M.	Winters	8/12/92	153.00		45.50	44.10	0.38	68.40	2.06	0.57	6.46	221.00	354.00	7.50	25.50				
50-08-101	Darring, B	Kennedy	1/22/92	29.80	2.26	7.70	95.00	*0.05	21.10	1.49	<0.01	5.80	73.60	271.00	6.95	18.70	6.78			
50-08-202	Darring, B	So. Carpenter	1/22/92	20.40	<1.39	9.28	113.00	<0.04	16.40	1.00	<0.01	78.70	107.00	207.00	7.13	18.70	7.00			
48-63-902	Darring, B	Witch	1/22/92	96.40	2.21	24.40	30.80	0.39	22.00	3.76	<0.01	10.20	63.20	331.00	7.56	16.10	0.20	-6.6	21.2	12823
48-64-303	Dees, C.	Pump Jack	1/22/92	121.00	2.05	56.30	65.40	0.62	83.20	2.18	<0.01	39.60	189.00	376.00	7.37	20.10	5.22	-9.7	94.4	476
48-56-805	Dees, J.		3/30/92	178.00	<1.54	81.20	88.90	0.54	178.00	0.94	<0.01	28.40	262.00	460.00	6.91	18.70	4.52	-8.4	79.5	1896
47-49-100	Garren, W.	Talc Mine	3/30/92	79.50	*1.52	56.70	104.00	1.07	76.00	0.84	<0.01	29.40	242.00	320.00	7.37	20.20	6.51	-9.4	103.3	Recent
47-49-101	Garren, W.	Big Mtn.	3/30/92	33.10	<1.54	15.60	85.10	0.07	11.60	0.42	<0.01	10.80	43.00	331.00	7.13	21.50	6.28	-11.8	109.9	Recent
47-49-102	Garren, W.	House	3/30/92	101.00	*1.49	47.40	53.80	0.53	39.70	0.69	<0.01	24.80	127.00	412.00	7.41	19.80	6.01	-10.1	108.5	Recent
51-01-503	King, C.	House	1/22/92	92.00	<1.39	2.76	7.32	0.22	4.84	2.42	<0.01	3.01	34.40	232.00	8.27	23.30	0.09	-4.7	2.2	31551
47-57-704	Koehn, R.		1/22/92	77.40	2.07	33.10	80.10	0.17	43.40	1.11	<0.01	9.02	110.00	386.00	7.09	21.10	7.69	-12.6	100.8	Recent
48-53-505	MERCO	Etholen	3/30/92	751.00	2.03	34.10	85.60	1.11	149.00	2.99	0.70	<0.10	1170.00	649.00	7.16	23.20	0.35	-6.1	12.7	17059
48-53-505	MERCO	Etholen	8/12/92	779.00		36.10	92.30	1.10	154.00	2.19	1.48	<0.80	1250.00	627.00	7.02	25.10	0.26			
48-64-302	Pioneer Talc		1/22/92	106.00	3.44	57.40	54.60	0.48	68.00	1.30	<0.01	30.90	217.00	310.00	7.43	19.10	3.11	-6.9	47.1	6224
48-64-602	Pioneer Talc	Office	1/22/92	161.00	4.62	108.00	140.00	0.70	145.00	1.27	<0.01	38.70	717.00	234.00	7.30	21.80	1.53	-7.0	23.5	11972
48-64-620	Southern Clay	Office	1/22/92	74.20	2.20	36.70	49.30	0.35	45.00	0.90	<0.01	14.50	98.90	320.00	7.43	21.40	0.42	-8.2	52.5	5327
48-54-404	Vance, B.			402.00	22.60	13.40	44.40	0.66	357.00	5.05	<0.01	15.10	289.00	328.00	7.28	31.40	0.68	-5.0	8.8	20091
48-54-404	Vance, B.		8/12/92	433.00		14.20	51.30	0.74	361.00	4.93	0.87	13.10	332.00	370.00	7.21	32.00				
48-45-901	MERCO	Ward	8/12/92	226.00		27.10	63.50	0.45	86.90	3.16	0.64	16.40	316.00	347.00	7.27	27.50	1.36			
48-53-803	Walker, J.		8/12/92	51.70		13.90	141.00	0.14	22.30	1.32	<0.25	1.86	158.00	361.00	7.17	20.60	1.73			
50-06-301	Love, D.	Red Light Mill	8/12/92	131.00		18.20	36.70	0.28	39.10	1.88	<0.25	4.74	164.00	274.00	7.64	27.30	0.08			
48-55-902	Dees, J.	House	8/12/92	56.70		33.80	58.20	0.26	20.30	0.90	<0.25	18.70	59.30	386.00	7.34	20.90				

data, coupled with the elevation of the potentiometric surface and the absence of springs or other evidence of discharge, suggest that eastern Eagle Flat may be connected hydrologically with Lobo Valley to the east.

The hydrochemical signature of ground water from Red Light Draw is similar to that of the mixed bicarbonate ground water from Eagle Flat and Green River Valley. This is based on analyses published by the Texas Water Development Board. Thirteen wells from this area were sampled during June and July, but analytical results are not yet available.

GEOPHYSICAL INVESTIGATIONS

Seismic Reflection and Refraction Studies

BEG conducted field geophysical studies to determine the geometry of the sedimentary basin in which the site is located and to examine the internal stratigraphy of the sediments that fill the basin. Results from these studies will be used to decipher the geologic history of the basin and to constrain hydrogeological models.

Three types of seismic data, refraction, reflection, and surface wave data, were collected at Faskin Ranch in 13 field days between May 21 and June 7, 1992. Refraction data, which are used to determine seismic velocities and thicknesses of subsurface layers, were collected at 6 sites at the ranch (fig. 15). Reflection data, which are used to construct continuous cross sections of the basin, were collected along four lines (LLFR1, 2, 3, and 4) that together extend for more than 3.7 mi (>6 km) (fig. 16). Surface wave data, which are used to determine physical properties of near-surface sediments, were collected from one site near the intersection of reflection lines LLFR1 and LLFR3. BEG is processing the refraction data, UTEP is processing the surface wave data, and BEG and UTEP are processing the reflection data using two different processing packages.

Layer velocities and thicknesses were obtained from all six refraction spreads (fig. 17). Layer 1, which is the surface layer, is characterized by seismic velocities of 1,230 to 1,395 ft/s

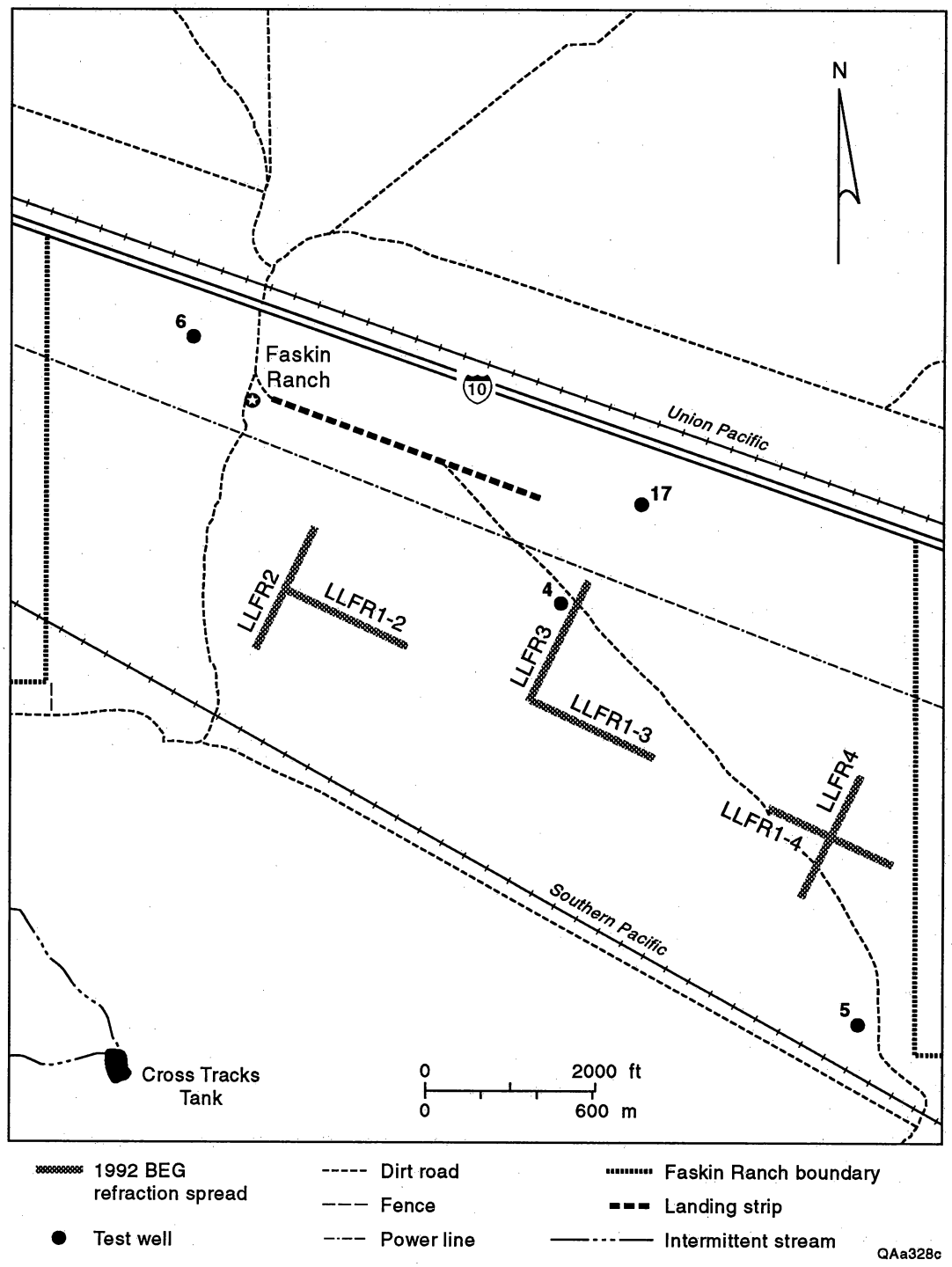

Figure 15. Map showing location of refraction spreads on the northern Faskin Ranch.

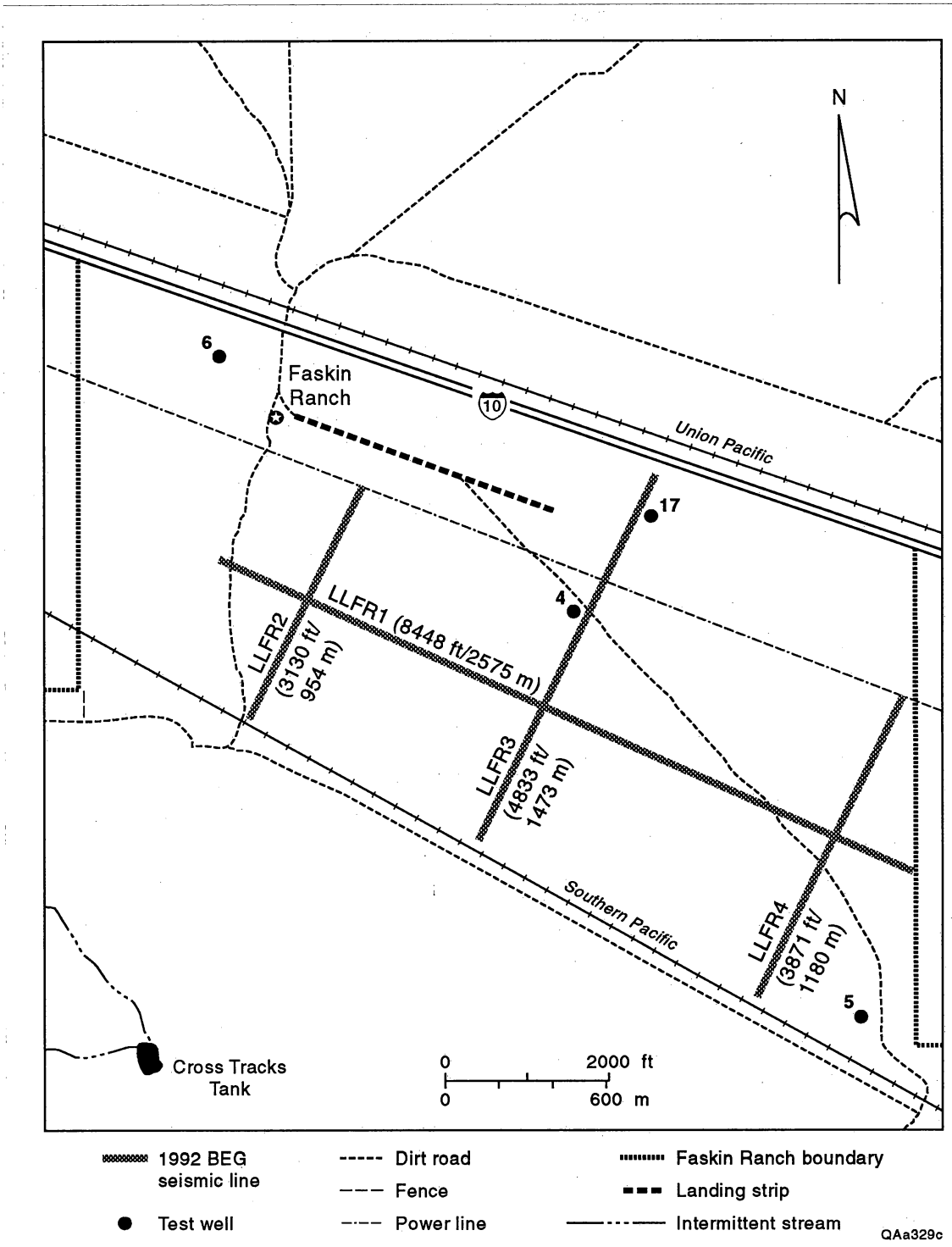

Figure 16. Map showing location of shallow reflection seismic lines on the northern Faskin Ranch.

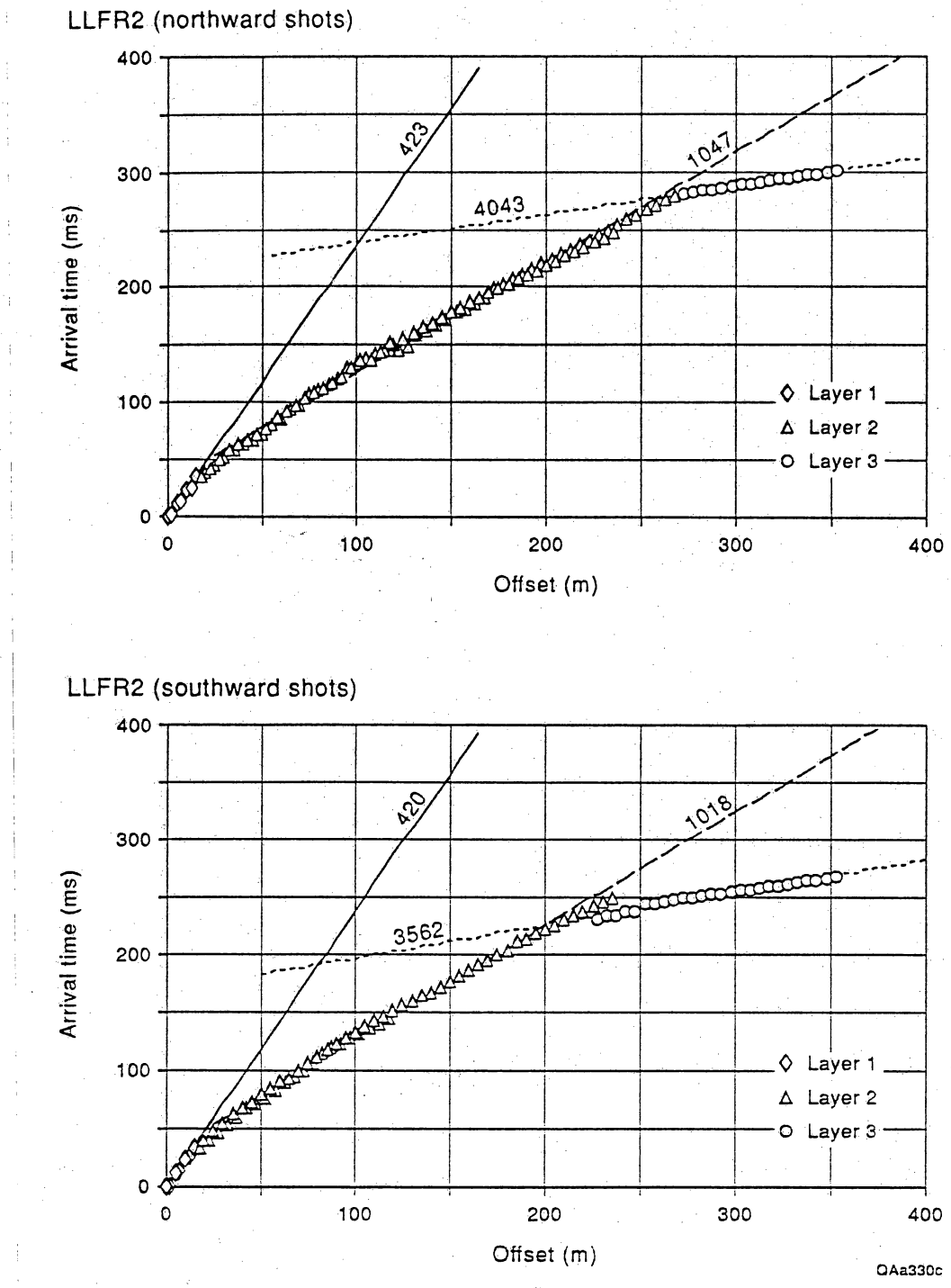

Figure 17. First-break times, layer assignments, and layer velocities for refraction spread LLFR2 (see fig. 16 for location). Layer velocities in m/s.

(375 to 425 m/s) and thicknesses of 16.4 to 32.8 ft (5 to 10 m). Layer 1 is underlain by layer 2, which has seismic velocities near 3,280 ft/s (1,000 m/s) and thicknesses (uncorrected for dip) ranging from 180 to 375 ft (55 to 114 m) across the site. Seismic velocities in layer 3 are significantly higher than those in the overlying basin fill layers; this layer represents bedrock. Depths to bedrock, also uncorrected for dip, range from 210 to 400 ft (64 to 121 m).

Reflection data augment refraction data by providing a continuous profile of subsurface interfaces rather than thickness and depth measurements at a single point. Reflection data collected by BEG have been corrected for elevation differences across the site, converted to industry-standard format, and are currently being processed at both UTEP and BEG. Preliminary processing of line LLFR2 indicates that the bedrock–basin fill boundary is visible, as is a reflecting horizon within the basin fill (fig. 18). Depth-to-bedrock estimates of 245 to 260 ft (75 to 80 m) made from LLFR2 reflection data are similar to an estimate of 295 ft (90 m) made from LLFR2 refraction data; both of these values are consistent with depths to bedrock determined at nearby boreholes. Similar concordance is expected at other sites where reflection and refraction data coincide.

At UTEP, preliminary processing has been completed for lines LLFR1 and LLFR3. The UTEP processing flow consists of several steps, including elevation correction, recovery of true trace amplitudes, noise reduction, predictive deconvolution, application of bandpass filters, moveout correction, and production of a common-depth-point (CDP) stacked section. Presently, parameters for CDP stacks and residual and refraction statics corrections are being investigated. In addition, strong surface wave energy recorded from test shots is being evaluated for input into a surface wave inversion algorithm. If the data are suitable, results from this procedure should produce a velocity-depth function on the basis of surface wave energy.

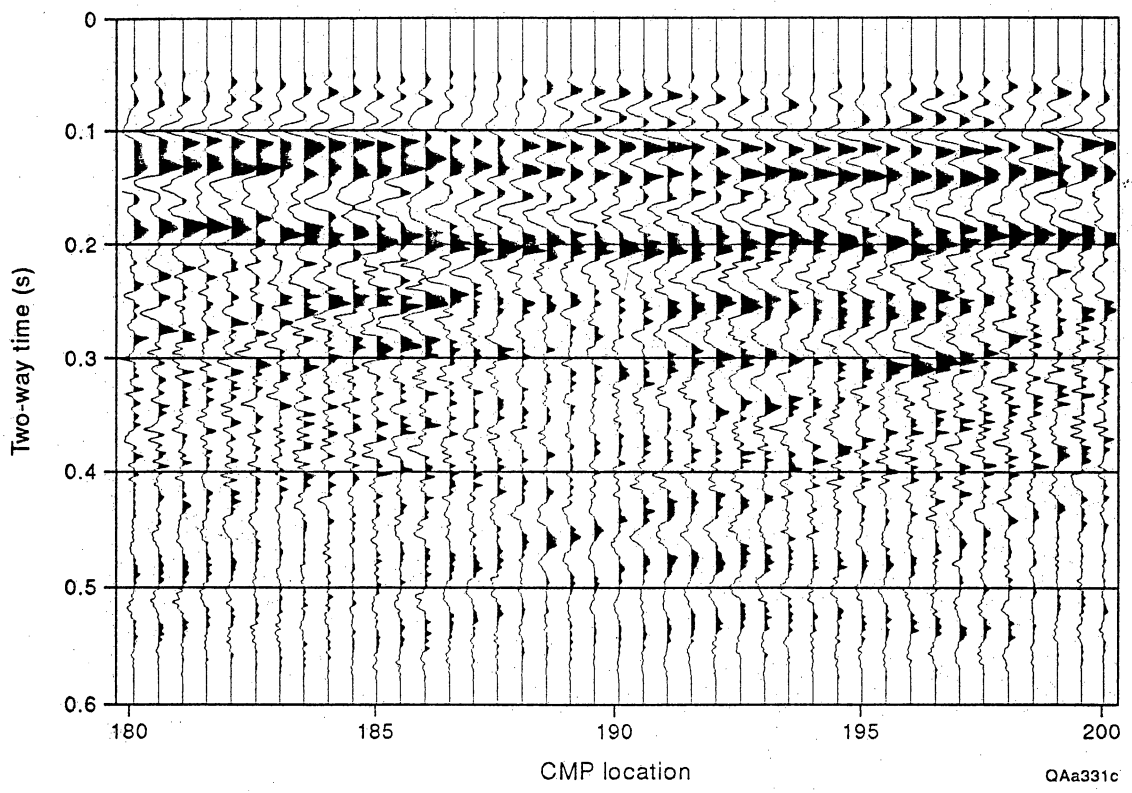

Figure 18. Sample seismic reflection section from line LLFR2 near where it crosses LLFR1-2 (see figs. 16 and 17 for location). Bedrock reflector can be seen at about 0.2 s; another reflector can be seen within the basin fill between 0.1 and 0.15 s. Seismic traces are 1.5 m apart.

Paleomagnetic Studies

Over geologic time, the Earth's magnetic field has changed its polarity many times. Such changes in the magnetic field are recorded in the rocks and sediments, and the timing of these changes has been carefully studied at many locations. By comparing the magnetic character, the paleomagnetism, of a sequence of sediments (such as those present at the proposed site) to the known timing of polarity changes, it is possible to interpret the ages of the sediments. These ages are important because they allow us to infer rates of sedimentation and other processes important to our understanding of the proposed site.

UTEP has collected samples from cores drilled as part of this project (boreholes YM-1 to YM-7), and analyzed their paleomagnetic character. The following is a discussion of the initial results from the analysis of these samples.

Magnetic susceptibility measurements on all samples have been completed, and demagnetization of most of the samples is also complete. Remaining work will involve a few stronger demagnetization steps for individual samples of unexpected polarity (for example, single samples of one polarity that occur within a well-defined zone of the opposite polarity), and samples that appear to occur at reversal boundaries.

Magnetic susceptibility measurements give generally strong values of 10^{-3} to 10^{-4} SI (susceptibility is dimensionless, so it has no units). The strength of the measurements indicates the presence of moderate amounts of magnetite in the samples.

Both alternating field (AF) and thermal demagnetization techniques worked well. AF demagnetization normally reduced the magnetic intensity of individual samples to values of less than 10 percent natural remnant magnetism (NRM). This suggests that magnetite is the main carrier of the NRM in the samples. Thermal demagnetization of samples reduced the magnetic intensity of samples to less than 10 to 15 percent NRM by 590°C, but directions remained stable, with continuing reduction of intensity, up to 690°C. Continuing stability of the NRM directions above the Curie point of magnetite (583°C) indicates that a second mineral,

hematite, is also contributing to the NRM. Since the magnetization directions remain stable above the magnetite Curie point, the samples probably acquired their original directions of magnetization from a combination of detrital magnetite and hematite at the time of deposition and no significant overprinting of directions has occurred.

The thermal demagnetization of the samples produced a significant amount of noxious fumes and blackening of the samples up to 450°C, indicating the presence of organic material in the samples. This, together with the demagnetization results (that suggest that any hematite present is primary and detrital and not formed as a result of secondary alteration of magnetite) may suggest that there has been little or no significant flow of oxidizing fluids (that is, ground water) through the sediments sampled in this study.

The final magnetic polarity stratigraphy will depend on data reduction that is now in progress. However, on the basis of the raw data, it is possible to identify 11 major and 4 single-sample polarity intervals in the longest core (YM-6). The second longest core (YM-4) records 8 major and 3-single sample polarity intervals. Both cores can be reasonably correlated to one another, assuming the borehole YM-4 locality had a slightly higher sedimentation rate than the borehole YM-6 locality. Together, they indicate a minimum of 4.0 mya of deposition and possibly more than 4.35 mya of deposition within this basin at these localities. Cores YM-3 and YM-7 also appear to correlate well with the upper halves of YM-4 and YM-6. Cores YM-1 and YM-2 are so short that they add little information. The results from borehole YM-5 are problematic because the core includes sections that are too poorly consolidated to be used for paleomagnetic analysis.

Although coring started as close as 11 ft (3.4 m) to the surface, samples of normal polarity (Brunhes) at the top of each core are scarce. The uppermost samples from borehole YM-2 are reversed, whereas cores YM-3, YM-4, YM-5, and YM-6 produced only two normal polarity samples above the Matuyama. Results from borehole YM-7 provide the best evidence for the Brunhes because the first 10 samples, collected at short sampling intervals, are all of normal polarity. The greatest depth of the Brunhes in any core is only 24.5 ft (7.5 m), and its greatest

thickness, as represented by these cores, is only 13.3 ft (4.1 m). If cores from boreholes YM-4 and YM-6 have maximum ages of approximately 4.35 mya, then the average sedimentation rates are 0.6 to 0.7 inches/10^3 yr (16.3 to 17.5 mm/10^3 yr).

REFERENCES

Albritton, C. C., Jr., and Smith, J. F., Jr., 1965, Geology of the Sierra Blanca area, Hudspeth County, Texas: U.S. Geological Survey Professional Paper 479, 131 p.

Baumgardner, R. W., Jr., and Scanlon, B. R., in press, Surface fissures in the Hueco Bolson and adjacent basins, West Texas: The University of Texas at Austin, Bureau of Economic Geology Geological Circular 92-2, 40 p.

Barnes, J. R., Shlemon, R. J., and Slemmons, D. B., 1989, The Amargosa fault: a previously unstudied major active fault in northern Chihuahua, Mexico (abs.): Association of Engineering Geologists Abstracts and Program, 32d Annual Meeting, p. 50–51.

Bostwick, D. L., 1953, Structural geology of northern Indio Mountains, Hudspeth County, Texas: University of Texas, Austin, Master's thesis, 56 p.

Collins, E. W., and Raney, J. A., 1990, Neotectonic history and structural style of the Campo Grande fault, Hueco Basin, Trans-Pecos Texas: The University of Texas at Austin, Bureau of Economic Geology Report of Investigations No. 196, 39 p.

_____ 1991a, Tertiary and Quaternary structure and paleotectonics of the Hueco Basin, Trans-Pecos Texas, and Chihuahua, Mexico: The University of Texas at Austin, Bureau of Economic Geology Geological Circular 91-2, 44 p.

_____ 1991b, Neotectonic history and geometric segmentation of the Campo Grande fault: a major structure bounding the Hueco Basin, Trans-Pecos Texas: Geology, v. 19, no. 5, p. 483–496.

Coordinación General de los Servicios Nacionales de Estadistica, 1982, San Antonio El Bravo: Carta Geologica, Dirección General de Geografia, scale 1:250,000.

DeFord, R. K., 1969, Some keys to the geology of northern Chihuahua, *in* Cordoba, D. A., Wengerd, S. A., Shomaker, John, eds., Guidebook of the border region: New Mexico Geological Society, Twentieth Field Conference, p. 61–65.

DeFord, R. K., and Bridges, L. W., 1959, Tarantula Gravel, northern Rim Rock country, Trans-Pecos Texas: Texas Journal of Science, v. 11, p. 286–295.

Doser, D. I., 1987, The 16 August 1931, Valentine, Texas, earthquake: evidence for normal faulting in West Texas: Bulletin of the Seismological Society of America, v. 77, p. 2005–2017.

Dumas, D. B., Dorman, H. J., and Latham, G. V., 1980, A reevaluation of the August 16, 1931, Texas earthquake: Bulletin of the Seismological Society of America, v. 70, no. 4, p. 1171–1180.

Gates, J. S., White D. E., Stanley, W. D., and Ackermann, H. D., 1980, Availability of fresh and slightly saline ground water in the basins of westernmost Texas: Texas Department of Water Resources, Report 256, 108 p.

Gile, L. H., Hawley, J. W., and Grossman, R. B., 1981, Soils and geomorphology in the Basin and Range area of southern New Mexico—guidebook to the Desert Project: New Mexico Bureau of Mines & Mineral Resources, Memoir 39, 222 p.

Gile, L. H., Peterson, F. F., and Grossman, R. B., 1966, Morphological and genetic sequences of carbonate accumulation in desert soils: Soil Science, v. 101, no. 5, p. 347–360.

Gries, J. G., 1979, Problems of delineation of the Rio Grande rift into the Chichuahua Tectonic Belt of northern Mexico, *in* Ricker, R. E., ed., Rio Grande rift: tectonics and magmatism: Washington, D. C., American Geophysical Union, p. 107–113.

_____ 1980, Laramide evaporite tectonics along the Texas-northern Chihuahua border, *in* Dickerson, P. W., Hoffer, J. M., and Callender, J. F., eds., Trans-Pecos region, southeastern New Mexico and West Texas: New Mexico Geological Society, Annual Field Conference Guidebook No. 31, p. 93–100.

Hawley, J. W., 1975, Quaternary history of Doña Ana County region, south-central New Mexico, *in* Seager, W. R., Clemons, R. E., and Callender, J. F., eds., Las Cruces country: New Mexico Geological Society, Annual Field Conference Guidebook No. 26, p. 139–140.

Hay-Roe, Hugh, 1957, Geology of Wylie Mountains and vicinity, Culberson and Jeff Davis Counties, Texas: University of Texas, Austin, Bureau of Economic Geology, Geologic Quadrangle Map No. 21, scale 1:63,360.

Henry, C. D., and Price, J. G., 1985, Summary of the tectonic development of Trans-Pecos Texas: The University of Texas at Austin, Bureau of Economic Geology Miscellaneous Map No. 36, 8 p.

_____ 1986, Early Basin and Range development in Trans-Pecos Texas, and adjacent Chihuahua: magmatism and orientation, timing, and style of extension: Journal of Geophysical Research, v. 91, no. B6, p. 6213–6224.

Jachens, R. C., and Holzer, T. L., 1979, Geophysical investigations of ground failure related to ground-water withdrawal—Picacho basin, Arizona: Ground Water, v. 17, no. 6, p. 574–585.

Jones, B. R., and Reaser, D. F., 1970, Geology of southern Quitman Mountains, Hudspeth County, Texas: The University of Texas at Austin, Bureau of Economic Geology Geologic Quadrangle Map No. 39, scale 1:48,000, text 24 p.

Keaton, J. R., Shlemon, R. J., Slemmons, D. B., Barnes, J. R., and Clark, D. G., 1989, The Amargosa fault: a major late Quaternary intraplate structure in northern Chihuahua,

Mexico (abs.): Geological Society of America, Abstracts with Programs, v. 21, no. 6, p. A148.

King, P. B. 1935, Outline of the structural development of Trans-Pecos Texas: American Association of Petroleum Geologists Bulletin, v. 19, p. 221–261.

_____ 1965, Geology of the Sierra Diablo Region, Texas: U.S. Geological Survey Professional Paper 480, 185 p.

Machette, M. N., 1985, Calcic soils of the southwestern United States, *in* Weide, D. L., ed., Soils and Quaternary geology of the southwestern United States: Geological Society of America Special Paper 203, p. 1-21.

Muehlberger, W. R., Belcher, R. C., and Goetz, L. K., 1979, Quaternary faulting in Trans-Pecos Texas: Geology, v. 6, no. 6, p. 337–340.

_____ 1985, Quaternary faulting in Trans-Pecos Texas (abs.), *in* Dickerson, P. W., and Muehlberger, W. R., eds., Structure and tectonics of Trans-Pecos Texas: West Texas: Geological Society Publication 85-81, p. 21.

Price, J. G., Henry, C. D., and Standen, A. R., 1983, Annotated bibliography of mineral deposits in Trans-Pecos Texas: The University of Texas at Austin, Bureau of Economic Geology Mineral Resource Circular No. 73, 108 p.

Price, J. G., Henry, C. D., Standen, A. R., and Posey, J. S., 1985, Origin of silver-copper-lead deposits in red-bed sequences of Trans-Pecos Texas: Tertiary mineralization in Precambrian, Permian, and Cretaceous sandstones: The University of Texas at Austin, Bureau of Economic Geology Report of Investigations No. 145, 65 p.

Sandford, A. R., and Toppozada, T. R., 1974, Seismicity of proposed radioactive waste disposal site in southeastern New Mexico: New Mexico Bureau of Mines and Mineral Resources Circular 143, 15 p.

Scanlon, B. R., 1992, Environmental and applied tracers as indicators of liquid and vapor transport in the Chihuahuan Desert, Texas: The University of Texas at Austin, Bureau of Economic Geology Report of Investigations No. 207, 51 p.

Scanlon, B. R., Wang, F. P., and Richter, B. C., 1991, Field studies and numerical modeling of unsaturated flow in the Chihuahuan Desert, Texas: The University of Texas at Austin, Bureau of Economic Geology Report of Investigations No. 199, 56 p.

Seni, S. J., 1992, Mineral and geothermal resources in the Eagle Flat region, West Texas: The University of Texas at Austin, Bureau of Economic Geology, report prepared for the Texas Low-Level Radioactive Waste Disposal Authority under contract no. IAC (92-93)-0910, 33 p.

Twiss, P. C., 1959, Geology of Van Horn Mountains, Texas: University of Texas, Austin, Bureau of Economic Geology Geologic Quadrangle Map No. 23, scale 1:48,000.

Underwood, J. R., Jr., 1963, Geology of Eagle Mountains and vicinity, Hudspeth County, Texas: University of Texas, Austin, Bureau of Economic Geology Geologic Quadrangle Map No. 26, scale 1:48,000, 32 p. text.

Wermund, E. G., 1992, Analysis of lineaments in the Eagle Flat study area, Hudspeth County, Texas: The University of Texas at Austin, Bureau of Economic Geology, report prepared for the Texas Low-Level Radioactive Waste Disposal Authority under contract no. IAC (92-93)-0910.

APPENDICES

Appendix I. Summary of Preliminary Investigations of the Quaternary Faults, Eagle Flat Study Area and Adjacent Region

E. W. Collins and J. A. Raney

Introduction

Geologic investigations of faults active during the Quaternary (present to ~2 mya) provide important data for seismic risk studies. Faults that have had Quaternary movement are being identified and mapped. Other geologic data useful for evaluating the seismic risk of possible earthquakes are being collected. These studies are based on aerial photograph interpretations and initial field studies. Because the investigations are ongoing, the data presented in this report are preliminary. The study area includes a region more than 50 km (>31 mi) from the Eagle Flat area, designated by the Texas Legislature, and the proposed repository site within Faskin Ranch (fig. 10). The study region contains intermontane basins and associated normal faults that have formed in response to Basin and Range extensional tectonism that began about 24 mya (Henry and Price, 1985; 1986).

Aerial photographs used in this study are: (1) 1991 black-and-white photographs, 1:6,000 scale; (2) 1980 color photographs, 1:24,000 scale, (3) 1972 black-and-white photographs, scales 1:32,000 and 1:26,000; (4) 1963 black-and-white photographs, scale 1:28,000; (5) 1957 black-and-white photographs, 1:62,000; and (6) 1948 black-and-white photographs, scale 1:43,000. We are also using U.S. Geological Survey Van Horn–El Paso and Marfa 2-degree topographic maps (scale 1:250,000), the Van Horn, Marfa, and El Paso Joint Operations Graphic (ground) maps (scale 1:250,000), Geological Survey 7.5-minute quadrangle maps (scale 1:24,000), and several Secretaria de Programiación y Presupuesto topographic maps of Chihuahua, Mexico, including the Guadalupe D. B., Esperanza, Las Palmas, Porvenir, El Consuelo, Banderas, and Cajoncitos sheets

(scale 1:50,000). Distances of faults to a reference point on the Faskin Ranch, latitude 105°15' and longitude 31°07'30", are reported. Scarp heights, measured using an Abney level, usually do not reflect the exact amount of vertical offset across faulted geomorphic surfaces because the geomorphic surfaces are sloping, the scarps are eroded, and colluvial deposits often are deposited on faulted downthrown surfaces.

Precise ages of faulted Quaternary (present to ~2 mya) and Tertiary (~2 to 66.4 mya) deposits have not been determined because these deposits have few materials suitable for accurate dating. At some localities we have estimated ages of Quaternary deposits, associated with fault scarps or occurring near projections of fault traces, to be middle Pleistocene (250,000 to 900,000 B.P.), upper Pleistocene (10,000 to 250,000 B.P.), and Holocene (present to 10,000 B.P.). These ages are estimated on the basis of field stratigraphic relationships, the degree of calcic soil development (Gile and others, 1966, 1981; Machette, 1985), and correlation with similar units in New Mexico and western Trans-Pecos Texas (Hawley, 1975; Gile and others, 1981; Collins and Raney, 1990, 1991a). In the study area, middle Pleistocene deposits having a stage IV to stage V pedogenic caliche are probably no older than 500,000 yr.

The following discussion briefly describes preliminary geologic observations of faults that have been active during the late Tertiary to Quaternary. Table 1 highlights some of the fault characteristics.

Northwest Eagle Flat Basin

Fault scarps do not occur in the middle Pleistocene to Holocene surficial sediments of the northwest Eagle Flat area, the locality of the proposed repository. Preliminary interpretations of data from drill holes and the bedrock geology surrounding this basin do not indicate the presence of any subsurface faults with large throw at the base of the Tertiary basin-fill deposits (top of bedrock) beneath or near the proposed repository. We anticipate that data from geophysical surveys will provide evidence of the presence or absence of faults in basin-fill sediments. Basin-fill thickness is

locally more than 180 m (>600 ft) although mostly less than 150 m (<500 ft), indicating that late Tertiary Basin and Range faulting and coincident basin sedimentation were not as active in the northwest Eagle Flat basin as in other basins of Trans-Pecos Texas.

Southeast Eagle Flat Basin

The southeast Eagle Flat Basin has as much as 600 m (2,000 ft) of basin fill (Gates and others, 1980) and the south part of the basin is bounded by two normal faults that are expressed at the surface, the West Van Horn Mountains fault and the East Eagle Mountains fault.

West Van Horn Mountains Fault

The west-dipping West Van Horn Mountains fault (fault 9, fig. 10) strikes northward at N30°W to N15°E at the base of the Van Horn Mountains and is a well-expressed part of the regional Rim Rock fault (DeFord, 1969). Muelberger and others (1979) found no evidence of Quaternary displacement along this fault. Along most of the fault, Quaternary-Tertiary basin fill is in contact with limestone and sandstone bedrock of the mountains and, although the contact/fault trace is sharp, no scarp is distinct. The northwestern 2.5 km (1.5 mi) of the fault trace is a gentle, dissected scarp with a slope angle of about 7°. Here the fault separates gravel deposits of unknown age on the upthrown block with Quaternary and Tertiary sand and gravel deposits on the downthrown block. A middle Pleistocene pediment surface having a stage IV pedogenic caliche occurs on the downthrown side of the fault. Locally the middle Pleistocene deposits are covered by younger windblown silt and sand, and in some places the older deposits are eroded and younger sediments have been deposited. The upthrown gravel deposits form well-dissected hills with relief as much as 30 m (100 ft). Locally, on the upthrown block, a remnant pediment surface of unknown age exists at the scarp. Its height above the middle Pleistocene surface on the downthrown fault block is 2.4 m (7.8 ft).

Even though this fault may not have had surface rupture during the Quaternary, we include it in this report because part of the fault does exhibit a subtle scarp in basin-fill deposits. The length of the West Van Horn Mountains fault is 27 km (16.7 mi) and the closest distance between this fault and the Faskin Ranch reference point is 38.5 km (24 mi). The surface trace of the fault dies out northward and there is no surface evidence of a northwest-striking fault flanking the southwest side of the Carrizo Mountains. South of the West Van Horn Mountains fault, strands of the Rim Rock fault displace bedrock.

East Eagle Mountains Fault

On the west side of the southeast Eagle Flat basin a short, 0.5-km-long (0.3-mi) scarp of the East Eagle Mountains fault (fault 6, fig. 10) strikes N10°-20°W and dips eastward. This fault is inferred to be as long as 5 km (3 mi), even though most of the inferred length is covered and only a short part of the fault, 0.5 km (0.3 mi), has surface expression. The fault is on the Pinyon Ranch, which is not currently accessible for ground investigations. Faulted deposits are interpreted to be Quaternary and probably middle Pleistocene on the basis of aerial photograph study and ground investigations conducted several kilometers to the north and to the east-northeast. The lateral extent of this fault was interpreted on the basis of the lack of the scarp in northern and southern surficial deposits that have the same aerial photograph characteristics as the faulted surficial deposits. The closest distance between this fault and the Faskin Ranch reference point is 32 km (20 mi).

Green River Basin

South of the southeast Eagle Flat is the north-trending Green River basin that has more than 600 m (>2,000 ft) of Quaternary–Tertiary basin fill deposits in its deepest part (Gates and others, 1980). Subtle scarps of three faults occur in the north part of this basin, but it is unclear whether these faults were active during the Quaternary.

Indio Fault

The Indio fault (fault 18, fig. 10) strikes N20°-45°W, and Bostwick (1953) reported that this fault dips 75° southwest. Its total length is 20 km (12.4 mi), although only the southeastern 6 km (3.7 mi) of the fault exhibits a mappable trace where Quaternary(?)–Tertiary gravel deposits are faulted against more resistant bedrock comprised of Cretaceous limestone and sandstone and Tertiary trachyte and tuff. Underwood (1963) thought that the gravel deposits on the downthrown block resulted from late Tertiary fault movement and may be equivalent to the Tertiary Tarantula gravel, which occurs east of the Green River basin (DeFord and Bridges, 1957). Even though this fault may not have been active since late Tertiary, we included it in this study because a scarp is preserved. The closest distance to the Faskin Ranch reference point is 50 km (31 mi).

China Canyon Fault

The China Canyon fault (fault 19, fig. 10) strikes N10°-20°W, dips eastward, and is 1 to 1.5 km (0.6 to 0.9 mi) long. The scarp is subtle and dissected, and Quaternary–Tertiary basin-fill deposits are faulted against Tertiary Tarantula gravel. Twiss (1959) mapped an inferred fault trace in the same area, although he inferred a length of 8.8 km (5.5 mi). We have not identified a scarp along most of this inferred length. This fault is included in the study because a scarp exists, although it is unknown whether the faulted basin-fill silt, sand, and gravel in this area is Tertiary or Quaternary. Thus, this fault may have been inactive since late Tertiary. The closest distance to the Faskin Ranch reference point is 52 km (32.3 mi). The China Canyon fault is en echelon to the Green River fault (fault 20, fig. 10). These faults probably have had different rupture histories because 2.4 km (1.5 mi) separates the two faults, and the Green River fault bounds a deeper part of the basin (>600 km [>2,000 ft] basin fill) than the China Canyon fault (basin fill on hanging-wall block).

Green River Fault

The Green River fault (fault 20, fig. 10) strikes N15°-30°W, dips west- southwest and is 9 km (5.6 mi) long. It is well dissected and is composed of three main subtle scarps that are between 1.5 and 2 km long. Quaternary–Tertiary basin-fill deposits are faulted against Tertiary Tarantula gravel. Like the China Canyon fault, it is unknown whether the Green River fault has ruptured since the late Tertiary. The Green River fault is included in this study because a subtle scarp exists. The closest distance to the Faskin Ranch reference point is 52 km (32.3 mi).

Red Light Bolson

The northwest-trending Red Light bolson lies southwest and south of the proposed Eagle Flat repository. The bolson contains several southwest-dipping Quaternary fault scarps along its east margin, and one of these is the Quaternary fault scarp closest to the proposed repository. Quaternary–Tertiary basin fill is thickest, more than 600 m (>2,000 ft) thick (Gates and others, 1980), at the southeast part of the bolson.

West Eagle Mountains–Red Hills Fault

The West Eagle Mountains–Red Hills Fault (fault 1, fig. 10) consists of a dissected 1.5-km-long (0.9-mi) scarp located west of the Eagle Mountains and two en echelon dissected scarps, 7 km (4.3 mi) and 1 km (0.6 mi) long, located west of Red Hills. This fault could be as long as 40 km (24.8 mi) if surface expression of the fault has been eroded and the trace is covered along the west margin of Devils Ridge and most of the west edge of the Eagle Mountains. This fault strikes N35°-55°W. The Quaternary–Tertiary basin fill west of the Eagle Mountains is about 300 m (~1,000 ft) thicker than the basin fill west of Red Hills, suggesting different fault histories.

The scarp closest to the proposed repository is 13.5 km (8.3 mi) south- southwest of the Faskin Ranch reference point. This scarp, west of Red Hills, is very subtle, with a maximum scarp-slope

angle of only 4° and scarp heights between 1.4 and 4 m (4.6 to 13 ft). The faulted pediment deposits, probably middle Pleistocene, have a gravelly stage IV pedogenic caliche that is locally as much as 0.6 m (2 ft) thick. These deposits are offset between 1 and 2.5 m (3 and 8 ft) along the 7-km-long (4.3 mi) scarp.

The projected trace of the West Eagle Mountains–Red Hills fault has no surface expression where it is covered by upper Pleistocene deposits, with a stage II to III pedogenic calcic horizon and younger, probably Holocene, deposits. These upper Pleistocene and younger deposits do not appear to be faulted. The Faskin Ranch reference point is as close as 10.5 km (6.5 mi) to the inferred trace of the fault.

West Indio Mountains Fault

The West Indio Mountains fault (fault 3, fig. 10) separates the Indio Mountains from the south part of the Red Light bolson. This fault consists of several strands, strikes N30°-45°W, and is inferred to be as much as 47 km (29 mi) long. The scarp of one strand has a slope angle of 11° to 14° and a height as much as 3 m (10 ft). This fault strand displaces middle Pleistocene gravelly deposits having a stage IV caliche 1.8 to 2.5 m (6 to 8 ft). Local, probably upper Pleistocene deposits having a stage II to III calcic soil horizon are offset 0.9 m (3 ft) by this strand, indicating that individual surface rupture events may have ranged from about 1 to 1.5 m (3 to 5 ft). Another fault strand has a scarp with a slope angle of 18° and height of 3.5 m (11.5 ft). Probable upper Pleistocene gravel and sand deposits with boulders and cobbles have a stage II to III calcic soil and are offset 2.5 m (8 ft) by this fault. Erosion has removed much of the middle Pleistocene deposits along fault strands in this area; however, projections of probable middle Pleistocene deposits on the upthrown and downthrown fault blocks at several localities suggest as much as 3 to 5 m (10 to 15 ft) of maximum offset on these deposits.

The West Indio Mountains and the West Eagle Mountains–Red Hills faults are interpreted to have had separate rupture histories because (1) different thicknesses of basin-fill sediments occur on

the downthrown fault blocks, (2) the en echelon faults are separated by 4 km (2.5 mi), and (3) the West Indio Mountains fault displaces upper Pleistocene deposits, whereas no evidence exists that the West Eagle Mountains–Red Hills fault offsets upper Pleistocene deposits.

Nick Draw Fault

The short, 2.5-km-long (1.5-mi) Nick Draw fault (fault 5, fig. 10) occurs in the southwest part of the Red Light bolson. This fault strikes N10°- 15°E and dips west. About 1.2 km (0.7 mi) of the fault is a well-expressed scarp with erosion-resistant Tertiary ignimbrite of the upthrown block in contact against Quaternary–Tertiary basin-fill deposits of the hanging-wall block. Displacement during Quaternary is uncertain. The closest distance to the Faskin Ranch reference point is 29 km (18 mi).

Southeast Hueco Bolson

The southeast Hueco Bolson lies about 23 to more than 50 km (~14 to >31 mi) west of the proposed repository site and contains several well-expressed Quaternary faults (Collins and Raney, 1991a). The Hueco Bolson is larger and deeper than the other basins in our study area, suggesting it has had a more active Cenozoic structural history. Cenozoic basin fill is as thick as 2,850 m (9,350 ft) (Collins and Raney, 1991a).

Caballo Fault

The 48-km-long (29-mi-long) Caballo fault (fault 2, fig. 10) bounds the west flank of the Quitman Mountains and the east margin of the southeast Hueco Bolson. Jones and Reaser (1970) named a fault strand flanking the southern Quitman Mountains the Caballo fault, and Collins and Raney (1991a) described the probable northwest extension of the fault. The Caballo fault strikes N35°-55°W and dips southwest. Most of the surface trace is difficult to identify in the field and on

aerial photographs because the surface has been disturbed by erosion of the older sediments and deposition of younger alluvium. A well-dissected scarp at the northwest extension of the fault trace is probably the fault scarp, although it has not been excavated. Locally the scarp has a compound-slope angle, and its total height is 10.5 m (34 ft). The steep part of the compound slope is 15°. Collins and Raney (1991a) estimated as much as 24 m (78 ft) of possible offset for middle Pleistocene gravel deposits having stage IV–V caliche, although erosion of sediments makes precise measurement difficult. Offset of upper Pleistocene gravel deposits having a stage III calcic soil horizon is 7 m (23 ft), and younger upper Pleistocene deposits are not faulted. The approximate amount of vertical offset during the last surface rupture was about 1.7 m (~15.5 ft), assuming that the steep part of the compound scarp reflects the latest single rupture event. The closest distance to the Faskin Ranch reference point is 23 km (14.3 mi).

Ice Cream Cone Fault

The northwest-trending Ice Cream Cone fault (fault 4, fig. 10) strikes N15°-60°W, dips as much as 85° southwest, and has a surface trace of about 9 km (5.6 mi). This fault, described by Collins and Raney (1991a, their fault 12), offsets upper Pleistocene deposits 13.8 m (45 ft). Younger upper Pleistocene pediment gravel deposits are not faulted. The closest distance to the Faskin Ranch reference point is 29 km (18 mi).

Arroyo Diablo Fault

The 15-km-long (9.3-mi) Arroyo Diablo fault (fault 10, fig. 10) bounds the northeast margin of the southeast Hueco Bolson and is located about 5 to 6 km (3 to 4 mi) south of the Finlay Mountains. This fault, previously studied by Collins and Raney (1991a, their fault 10), strikes N30°-60°W, and in outcrop dips about 60° to 85° southwestward. Much of the trace of the Arroyo Diablo fault is covered by unfaulted sediments of late Pleistocene and Holocene age. Where a scarp is preserved in the middle Pleistocene deposits having stage IV to V pedogenic caliche, the scarp is

commonly covered by windblown sand. The most distinct, uncovered scarp has heights between 1.7 and 2.5 m (5.5 and 8 ft). This scarp has compound slopes that have angles as much as 15° at the steepest part of the scarp. Middle Pleistocene deposits having stage IV to V pedogenic caliche are displaced vertically as much as 3 m (10 ft). The approximate offset on the Arroyo Diablo fault during the last surface rupture was about 0.6 m (~2 ft), assuming that the steep parts of compound scarps reflect the latest single rupture event. The closest distance to the Faskin Ranch reference point is about 39 km (24 mi).

Amargosa Fault

The Amargosa fault (fault 11, fig. 10) flanks the northeast base of Sierra de San Ignacio, Sierra de la Amargosa, and Sierra San Jose del Prisco, and separates these mountains from the southwest edge of the southeast Hueco Bolson (Collins and Raney, 1991a, their fault 14). The Amargosa fault is composed of en echelon fault strands, and it has a surface trace of about 70 km (43 mi) and a regional strike of N40°-50°W. It dips northeast between 75° and 80° at the surface. The fault appears to exhibit mostly vertical offset where we studied it, although Barnes and others (1989) and Keaton and others (1989) reported grabenlike extensional features along the fault as evidence of lateral components of fault slip.

The Amargosa fault has the most distinct fault scarp in the southeast Hueco Bolson. Scarp-slope angles are between 19° and 27°. Scarp heights range between 32 and 2.8 m (105 and 9 ft), depending on the age of faulted sediments adjacent to the fault, because multiple ruptures have caused older Quaternary surfaces to be offset more than younger ones. Probably middle Pleistocene gravelly piedmont deposits having a pedogenic caliche displaying a stage IV to V morphology are offset 24 m (78 ft). Upper Pleistocene gravelly deposits with a stage III to IV pedogenic calcic horizon are offset as much as 6.5 m (21 ft), and younger upper Pleistocene gravelly deposits having a stage II pedogenic calcic horizon are offset 2.5 to 4.5 m (8 to 15 ft). Results of aerial photographic

mapping suggest that young, possibly Holocene deposits, may be offset at some localities along the Amargosa fault. The closest distance to the Faskin Ranch reference point is 41 km (25.4 mi).

Campo Grande Fault

The Campo Grande fault (fault 12, fig. 10) is a 45-km-long (28-mi) fault that bounds the northeast side of the Hueco Bolson (Collins and Raney, 1990, 1991a, their fault 15). This fault lies approximately midway between the Rio Grande and Diablo Plateau and is composed of en echelon fault strands that are 1.5 to 10 km (0.9 to 6 mi) long and that have strikes of N25°-75°W. Dips are between 60° and 89° southwest, and grooves on fault planes indicate mostly dip-slip movement. Subsurface studies indicate that the surface trace of the Campo Grande fault represents three en echelon subsurface fault segments that are each between 21 and 34 km (13 and 21 mi) long (Collins and Raney, 1991a, 1991b). The southeast part of the Campo Grande fault is the best surface expression of the fault. At this part of the fault, the heights of scarps range between 1.5 and 11.5 m (5 and 37 ft) and scarp slopes are 4° to 17°. Middle Pleistocene gravelly pediment deposits having a stage IV to V pedogenic caliche are offset as much as 10 m (32 ft). Upper Pleistocene gravel deposits having a stage III to IV pedogenic calcic horizon are offset as much as 3 m (10 ft). Younger upper Pleistocene gravel deposits having a stage II pedigenic calcic horizon are unfaulted. On the downthrown block of one fault strand, faulted calcic soil horizons (0.5 to 1.0 m [1.6 to 3 ft] thick; stage III morphology) that have vertical separations of 1 to 2 m (3 to 6.5 ft) indicate at least five episodes of movement, deposition, and surface stabilization since the middle Pleistocene. Maximum vertical offsets during single faulting events have been as much as 2 m (6.5 ft), judging from the vertical separations of these faulted, calcic soil horizons. Maximum vertical offset during the last faulting event was about 1 to 1.5 m (~3 to 5 ft). The closest distance to the Faskin Ranch reference point is 42 km (26 mi).

Arroyo Macho Fault

The short, 1.5-km-long (0.9-mi) Arroyo Macho fault strikes N30°-40°E and dips southeast (Collins and Raney, 1991a, their fault 11). Albritton and Smith (1965) measured 2 m (6.5 ft) of throw on middle Pleistocene gravelly pediment deposits having a stage IV to V pedogenic caliche. The closest distance to the Faskin Ranch reference point is 44 km (27.3 mi).

Acala Fault

The Acala fault (fault 26, fig. 10) strikes N40°-50°W, dips southwest, and has a surface trace of about 10 km (6.2 mi) (Collins and Raney, 1991a, their fault 7). The scarp has a single-slope angle of 9° (maximum), and the scarp is about 2.2 m (7.2 ft) high. Middle Pleistocene gravelly pediment deposits having a stage IV to V pedogenic caliche are estimated to be displaced about 18 m (59 ft). A shorter fault scarp having a surface trace of about 3 km (1.8 mi) (Collins and Raney, 1991a, their fault 8) is roughly en echelon to the longer scarp. The shorter scarp strikes N60°-70° and dips southwest. Its scarp has a single-slope angle of about 4°, and the scarp is only about 1 m (3 ft) high. Middle Pleistocene gravelly pediment deposits having a stage IV to V pedogenic caliche are offset about 4 m (13 ft). The closest distance to the Faskin Ranch reference point is 68 km (42 mi).

Llanos de Chilicote

Llanos de Chilicote lies in Chihuahua, Mexico, southwest of the proposed Eagle Flat repository. Two faults, the West Sierra de la Lagrina fault and the West Sierra Labra fault (faults 23 and 25, respectively, fig. 10), that bound mountain ranges of the Llanos de Chilicote region have been mapped as the contact between Quaternary–Tertiary gravel and sand deposits and Cretaceous bedrock (San Antonio El Bravo sheet; Coordinación General de los Servicios Nacionales de Estadistica, 1982). We do not currently have aerial photographs available, and we have not visited the area on the ground. We do not know whether fault scarps exist in this area. Gries (1979; 1980)

hypothesized that Cenozoic extension in this region may have reactivated older structures and caused flowage of thick evaporite sequences in the subsurface without causing surface rupture.

West Sierra de la Lagrina Fault

The West Sierra de la Lagrina fault (fault 23, fig. 10) has been mapped as a 41-km-long (25.4-mi) structure that strikes north-northwest at N5°-35°W and dips west (Coordinacion General de los Servicios Nacionales de Estadistica, 1982). The closest distance to the Faskin Ranch reference point is 61 km (40 mi).

West Sierra Labra Fault

The West Sierra Labra Fault (fault 25, fig. 10) has been mapped as a 22-km-long (13.6-mi) structure that strikes north-northwest at N0°-30°W and dips west (Coordinación General de los Servicios Nacionales de Estadistica, 1982). The closest distance to the Faskin Ranch reference point is 65 km (40 mi).

Salt Basin Graben System

The north-trending Salt Basin Graben System lies east of the proposed repository site. The graben system comprises a 200-km-long (124-mi) series of fault-bounded basins that include the Salt Basin, Wild Horse Flat, Michigan Flat, Lobo Valley, and Ryan Flat geographic areas (fig. A1). Tertiary–Quaternary basin fill is greater than 600 m (>2,000 ft) thick in some areas, although basin fill is mostly less than 300 m (<1,000 ft) thick (Gates and others, 1980).

East Flat Top Mountains Fault

Fifty-three kilometers (34 mi) north-northeast of the Faskin Ranch reference point, the East Flat Top Mountains fault (fault 21, fig. 10) bounds the west side of the Salt Basin. This 23-km-long

(14.2-mi) fault strikes northward at N25°W-N5°E and dips toward the east. A subtle scarp located at the north part of this fault has a scarp-slope angle of 3° and height of about 2.5 m (~8 ft). The faulted surficial sediments at this locality are unconsolidated, lacking a well-developed calcic soil horizon, and probably are of Holocene or late Pleistocene age. Offset of the faulted geomorphic surface is about 1.5 m (5 ft).

North Sierra Diablo Fault

The North Sierra Diablo fault (fault 22, fig. 10) strikes westward at N75°- 85°W, dips north, and separates the north part of Sierra Diablo from the Salt Basin. Most of the 13.5-km-long (8.3-mi) fault is covered or inferred, although a 4-km-long (2.5-mi) scarp occurs at the fault's east end. The closest distance to the Faskin Ranch reference point is 54 km (33.5 mi).

East Sierra Diablo Fault

The 37-km-long (23-mi) East Sierra Diablo Fault (fault 8, fig. 10) strikes northward at N10°W-N20°E, dips toward the east, and bounds the west side of the Salt Basin. This fault is composed of a series of about 11 en echelon fault strands, and about 60 percent of the fault's length is covered or inferred. The longest continuous scarp, located at the north part of the East Sierra Diablo fault and 5 km (3 mi) long, has a scarp-slope angle of 8° and height of 1.8 m (6 ft). The faulted surficial sediments consist of an upper, unconsolidated, 2-m-thick (6.5-ft) package of probably Holocene–upper Pleistocene boulder- to pebble-sized gravel and sand with a stage II to I calcic soil. This upper sediment package overlies an older, middle Pleistocene gravel and sand package with a greater than 1-m-thick (>3-ft) stage IV caliche horizon. Offset on the upper sediment package is about 1.5 m (5 ft), and offset on the lower, stage IV caliche horizon is unknown because the caliche horizon is not exposed in gullies on the downthrown fault block. It is unknown whether the entire length of this fault has had the same rupture history. The closest distance to the Faskin Ranch reference point is 37 km (23 mi).

West Delaware Mountains Fault

The West Delaware Mountains fault (fault 24, fig. 10) trends northwest at N25°-45°W, dips southwest, and separates the west flank of the Delaware Mountains from the deep part of the Salt Basin. This fault is about 64 km (~40 mi) long and consists of multiple en echelon fault strands. Most scarps along this fault are between 1 and 7 km (0.6 and 4.3 mi) long. At the north part of the West Delaware Mountains fault, multiple northwest-striking faults form a broad, 3- to 5-km-wide (1.8- to 3-mi) zone. The closest distance to the Faskin Ranch reference point is 64 km (40 mi).

East Carrizo Mountain–Baylor Mountain Fault

The 41-km-long (25.4-mi) Carrizo Mountain–Baylor Mountain fault (fault 7, fig. 10) separates the west side of Wild Horse Flat from the mountains the fault is named after. This fault strikes northeast at N10°-40°E and dips southeast. About 85 percent of this fault's length is covered and inferred. Three scarps along this fault are 1, 1.2, and 3 km (0.6, 0.7, and 1.8 mi) long. An eroded, subtle scarp, located west-southwest of Van Horn, has a scarp-slope angle of 5° and a height of 1.8 m (6 ft). The faulted pediment surface at this scarp has a stage IV pedogenic caliche suggesting a middle Pleistocene age for the faulted surficial deposits. Locally on the upthrown fault block, sandstone bedrock is at the surface. Offset on the middle Pleistocene deposits is 1.6 m (5.2 ft). The closest distance to the Faskin Ranch reference point is 37 km (23 mi).

Fay Fault

The Fay fault (fault 13, fig. 10) is a short, 4-km-long (2.5-mi) fault located at the north part of the Van Horn Mountains. This fault strikes north-northwest at N5°-20°W, dips east, and consists of two en echelon scarps. The scarp of the north part of this fault has a scarp-slope angle of 13° and height of 1.4 m (4.6 ft). Surficial middle Pleistocene deposits with stage IV pedogenic caliche are offset 1.2 m (4 ft). The closest distance to the Faskin Ranch reference point is 43 km (26.7 mi).

Deep Well Fault

The 1.3-km-long (0.8-mi) Deep Well fault (fault 15, fig. 10) is located at the north part of the Van Horn Mountains. We do not know whether this fault has ruptured during the Quaternary. Aerial photograph studies indicate that a sharp contact exists between Quaternary–Tertiary gravel deposits and Permian limestone along the fault's trace. The Deep Well fault strikes north- northwest at N10°-30°W, dips west, and the closest distance to the Faskin Ranch reference point is 47 km (29 mi).

East Van Horn Mountains–Sierra Vieja Fault
(Neal, Mayfield, and Sierra Vieja Segments)

The 61-km-long (38-mi) East Van Horn Mountains–Sierra Vieja fault (fault 16, fig. 10) bounds the West side of Lobo Valley and Ryan Flats. This fault consists of three distinct geometric segments, the Neal, Mayfield, and Sierra Vieja segments, which may have had different rupture histories. The East Van Horn Mountains–Sierra Vieja fault was also been called the Mayfield fault by Muehlberger and others (1979; 1985) and Doser (1987). We use the name Mayfield (after Twiss, 1959) to refer to the central segment of the long boundary fault.

The Neal fault (fault 16a, fig. 10), the north segment, strikes northward at N10°W-N25°E, dips east, and is about 18 km (~11 mi) long. This fault is comprised of a main 13.6-m-long (8.4-mi) scarp and several associated en echelon shorter scarps that are as much as 2 km (1.2 mi) long. One of the shorter scarps has a scarp-slope angle of 8° and a height of 2.2 m (7 ft). Offset of middle Pleistocene gravel capped with a stage IV pedogenic caliche is 1.8 m (6 ft) across this short scarp, which is near the north end of the Neal fault. The main 13.6-km-long (8.4-mi) scarp has a very distinct single slope with slope angles ranging between 14° and 22° and heights ranging between 1.6 and 4.8 m (5.2 and 15.7 ft). On the upthrown block, bedrock is shallow and locally is at the surface. Offset of middle Pleistocene deposits capped by a stage IV pedogenic caliche is at least 5 m (16.4 ft). The closest distance to the Faskin Ranch reference point is 48 km (30 mi).

The northwest-trending Mayfield fault (fault 16b, fig. 10) is the middle segment. It strikes N30°-55°W, dips northeast, and is about 20 km (~12.4 mi) long. It has a single slope scarp with scarp-slope angles ranging between 18° and 23° and heights between 4 and 7 m (13 and 23 ft). Similar to the Neal scarp, bedrock is shallow and locally at the surface on the upthrown fault block. Offset of middle Pleistocene deposits capped by a stage IV pedogenic caliche is as much as 6 m (19.6 ft). The closest distance to the Faskin Ranch reference point is 57 km (35.4 mi).

The Sierra Vieja fault (fault 16c, fig. 10) makes up the south segment of the fault series that bounds the west edge of Lobo Valley and Ryan Flat. The Sierra Vieja fault strikes northward at N30°W-N20°E, dips east, and is about 25 km (~15.5 mi) long. It consists of multiple en echelon strands. Some of the strands have 4.5-m-high (15-ft) compound scarps with steep scarp-slope angles as much as 20°. Similar to the Neal and Mayfield scarps, bedrock is shallow and locally is at the surface on the upthrown fault block. Offset of possible middle Pleistocene deposits is as much as 8.2 m (27 ft), and offset of possible late Pleistocene–Holocene deposits is as much as 3.5 m (11.4 ft). The last surface rupture may have been as much as 1.5 m (5 ft) if the steep part of the compound scarps was caused by a single rupture. The closest distance to the Faskin Ranch reference point is 77 km (48 mi).

West Wylie Mountains Fault

The West Wylie Mountains fault (fault 17, fig. 10) separates the north part of Lobo Valley from the Wylie Mountains and Canning Ridge. This fault is inferred to be about 20 km (~12.5 mi) long, and two 1-km-long (0.6-mi) scarps having Quaternary-Tertiary basin-fill on the hanging-wall block occur at the southwest flank of the Wylie Mountains and west flank of Canning Ridge. The north part of the fault has been mapped in bedrock at two localities (Hay- Roe, 1957). The West Wylie Mountains fault strikes N10°-30°W and dips southwest. The closest distance to the Faskin Ranch reference point is 48 km (30 mi).

Appendix II. Inventory of mineral occurrences, unique BEG number, locality name, location, commodity, district, and status.

BEG LOCALITY #	NAME	LATITUDE / LONGITUDE	COMMODITY	DISTRICT	TYPE
3004-333-801	Plata Verde Mine	N-30-52-38; W-104-55-18	Au, Pb, Ag	Van Horn Mts. Ag, Cu, Pb, Mn	Abandoned mine
3005-443-901	Black Hill (Dick Love Mine)	N-30-54-08; W-105-08-57	Mica	Eagle Mts. Pb, Zn, Ag, Cu	Abandoned mine
3005-443-902	Silver Eagle Mine	N-30-53-54; W-105-08-52	Pb, Ag, Zn	Eagle Mts. Pb, Zn, Ag, Cu	Abandoned mine
3005-443-903	Prospect 2	N-30-53-52; W-105-07-50	Pb	Eagle Mts. Pb, Zn, Ag, Cu	Abandoned mine
3005-443-904	Prospect 9	N-30-53-52; W-105-07-50	Ag	Eagle Mts. Pb, Zn, Ag, Cu	Abandoned mine
3005-444-101	Eagle Spring Coal Mine	N-30-59-15; W-105-06-10	Coal	Upper Cretaceous Coal Deposits	Abandoned mine
3005-444-102	Eagle Spring Fluorspar Mine	N-30-59-16; W-105-05-50	Fluorspar	Eagle Mts. Fluorspar Deposits	Abandoned mine
3005-444-103	Prospect 0, 10	N-30-59-17; W-105-05-40	Cu, Ag	Eagle Mts. Pb, Zn, Ag, Cu	Abandoned mine
3005-444-103	Unnamed prospect	N-30-59-17; W-105-05-40	Pb, Zn, Ag, Cu	Eagle Mts. Pb, Zn, Ag, Cu	Prospect
3005-444-501	Section 27 Prospect	N-30-57-11; W-105-03-49	Fluorspar	Eagle Mts. Fluorspar Deposits	Prospect
3005-444-502	Lucky Strike (Section 26) Prospect	N-30-56-47; W-105-03-10	Fluorspar	Eagle Mts. Fluorspar Deposits	Prospect
3005-444-503	Rhyolite Vein, Spar Valley	N-30-56-20; W-105-02-52	Fluorspar	Eagle Mts. Fluorspar Deposits	Abandoned mine
3005-444-504	Shaft 4, Spar Valley	N-30-56-01; W-105-03-05	Fluorspar	Eagle Mts. Fluorspar Deposits	Abandoned mine
3005-444-506	Tank Canyon Prospects	N-30-55-41; W-105-03-15	Fluorspar	Eagle Mts. Fluorspar Deposits	Prospect
3005-444-507	Syphon Canyon Prospects	N-30-55-24; W-105-02-49	Fluorspar	Eagle Mts. Fluorspar Deposits	Prospect
3005-444-601	prospect	N-30-56-42; W-105-01-28	Cu, Ag, Zn	Carrizo Mt. Cu, Ag, Zn	Abandoned mine
3005-444-602	Unnamed mine in Eagle Mts.	N-30-56-45; W-105-01-29	Cu, Ag, Zn	Carrizo Mt. Cu, Ag, Zn	Abandoned mine
3005-444-701	Fox 9 and 10 Prospects	N-30-54-10; W-105-06-21	Fluorspar	Eagle Mts. Fluorspar Deposits	Prospect
3005-444-702	Rocky Ridge Prospects	N-30-54-08; W-105-06-30	Fluorspar	Eagle Mts. Fluorspar Deposits	Prospect
3005-444-704	Section 45 Prospect	N-30-54-15; W-105-06-18	Fluorspar	Eagle Mts. Fluorspar Deposits	Prospect
3005-444-801	Ingram Prospect	N-30-54-15; W-105-03-10	Fluorspar	Eagle Mts. Fluorspar Deposits	Prospect
3005-444-802	Fox 1 and 3 Prospects	N-30-53-49; W-105-04-05	Fluorspar	Eagle Mts. Fluorspar Deposits	Prospect
3005-444-803	Divide Prospect	N-30-54-14; W-105-04-57	Fluorspar	Eagle Mts. Fluorspar Deposits	Prospect
3005-444-901	Fox 4 Prospects	N-30-54-38; W-105-02-20	Fluorspar	Eagle Mts. Fluorspar Deposits	Prospect
3005-444-902	Unnamed mine	N-30-54-36; W-105-01-48	Cu	Eagle Mts. Pb, Zn, Ag, Cu	Abandoned mine
3104-222-101	Unnamed quarry	N-31-06-50; W-104-59-56	Talc	Allamoore Talc District	Active mine
3104-222-102	Pit 3	N-31-06-40; W-104-59-05	Talc	Allamoore Talc District	Abandoned mine
3104-222-103	Cooper Hill (Rossman) Prospect	N-31-06-45; W-104-58-43	Cu, U	Van Horn-Allamoore Ag, Cu	Prospect
3104-222-104	Eagle Flat Mine	N-31-06-40; W-104-58-24	Talc	Allamoore Talc District	Active mine
3104-222-105	Bluebird Prospect	N-31-06-16; W-104-59-18	Ag	Van Horn-Allamoore Ag, Cu	Prospect
3104-222-106	Buck Spring Quarry	N-31-06-05; W-104-57-37	Talc	Allamoore Talc District	Active mine
3104-222-107	Garren II Pit	N-31-05-00; W-104-57-30	Talc	Allamoore Talc District	Active mine
3104-222-108	Unnamed prospects	N-31-06-30; W-104-58-15	Talc	Allamoore Talc District	Prospect
3104-222-201	Car Body Quarry	N-31-05-58; W-104-57-18	Talc	Allamoore Talc District	Active mine
3104-222-202	Pit 2	N-31-06-05; W-104-56-33	Talc	Allamoore Talc District	Abandoned mine
3104-222-203	Buck Springs Prospect	N-31-06-05; W-104-56-46	Ag	Van Horn-Allamoore Ag, Cu	Prospect
3104-222-204	Windmill Prospect	N-31-07-24; W-104-57-10	Talc	Allamoore Talc District	Abandoned mine
3104-222-401	Allamoore Quarry #89	N-31-03-52; W-104-57-41	Rhyolite	Aggregate	Active mine
3104-222-402	Unnamed Prospect	N-31-03-25; W-104-57-31	Cu, Ag	Carrizo Mt. Cu, Ag, Zn	Prospect
3104-222-403	Sawyer Prospect	N-31-02-34; W-104-57-51	Cu, Ag	Carrizo Mt. Cu, Ag, Zn	Abandoned mine
3104-222-501	Unnamed prospect	N-31-03-42; W-104-56-43	Cu, Ag	Carrizo Mt. Cu, Ag, Zn	Prospect
3104-222-502	Unnamed prospect	N-31-03-08; W-104-56-10	Cu, Ag	Carrizo Mt. Cu, Ag, Zn	Prospect
3104-222-503	Unnamed prospect	N-31-02-44; W-104-55-55	Cu, Ag	Carrizo Mt. Cu, Ag, Zn	Prospect
3104-222-601	Unnamed prospect	N-31-03-16; W-104-53-59	Gravel	Road metal, borrow pit	Borrow pit
3104-222-602	Neal Mann Prospect	N-31-03-21; W-104-54-46	Talc	Allamoore Talc District	Abandoned mine
3104-222-603	Unnamed prospect	N-31-02-34; W-104-54-23	Cu, Ag	Carrizo Mt. Cu, Ag, Zn	Prospect

Appendix II (cont.)

BEG LOCALITY #	NAME	LATITUDE / LONGITUDE	COMMODITY	DISTRICT	TYPE
3104-222-701	Unnamed prospect	N-31-01-25; W-104-59-45	Cu, Ag	Carrizo Mt. Cu, Ag, Zn	Prospect
3104-222-702	Unnamed prospect	N-31-02-20; W-104-58-50	Cu, Ag	Carrizo Mt. Cu, Ag, Zn	Prospect
3104-222-703	Unnamed prospect	N-31-01-18; W-104-58-02	Cu, Ag	Carrizo Mt. Cu, Ag, Zn	Prospect
3104-222-704	Unnamed prospect	N-31-01-30; W-104-58-05	Cu, Ag	Carrizo Mt. Cu, Ag, Zn	Prospect
3104-222-705	Unnamed prospect	N-31-01-22; W-104-57-55	Cu, Ag	Carrizo Mt. Cu, Ag, Zn	Prospect
3104-222-801	Maltby (Knight) Prospect	N-31-02-13; W-104-55-42	Cu, Ag, Au	Carrizo Mt. Cu, Ag, Zn	Prospect
3104-222-802	Unnamed prospect	N-31-02-18; W-104-56-35	Cu, Ag	Carrizo Mt. Cu, Ag, Zn	Prospect
3104-222-803	Unnamed prospect	N-31-00-52; W-104-55-06	Cu, Ag	Carrizo Mt. Cu, Ag, Zn	Prospect
3104-222-804	Unnamed prospect	N-31-01-13; W-104-55-53	Cu, Ag	Carrizo Mt. Cu, Ag, Zn	Prospect
3104-222-805	Unnamed prospect	N-31-01-41; W-104-56-40	Cu, Ag	Carrizo Mt. Cu, Ag, Zn	Prospect
3104-222-806	Unnamed prospect	N-31-00-26; W-104-57-06	Cu, Ag	Carrizo Mt. Cu, Ag, Zn	Prospect
3104-222-807	Unnamed prospect	N-31-02-28; W-104-56-40	Cu-Ag	Carrizo Mt. Cu, Ag, Zn	Prospect
3104-222-808	Unnamed prospect	N-31-02-27; W-104-55-30	Cu, Ag	Carrizo Mt. Cu, Ag, Zn	Prospect
3104-222-809	Unnamed prospect	N-31-01-22; W-104-55-14	Cu, Ag	Carrizo Mt. Cu, Ag, Zn	Prospect
3104-222-901	Unnamed prospect	N-31-02-07; W-104-53-04	Gravel	Road metal, borrow pit	Borrow pit
3104-222-902	Unnamed prospect	N-31-01-58; W-104-52-38	Gravel	Road metal, borrow pit	Borrow pit
3104-222-903	Unnamed prospect	N-31-02-22; W-104-54-30	Cu, Ag	Carrizo Mt. Cu, Ag, Zn	Prospect
3104-222-904	Unnamed prospect	N-31-02-07; W-104-53-51	Cu-Ag	Carrizo Mt. Cu, Ag, Zn	Prospect
3104-222-905	Unnamed prospect	N-31-02-18; W-104-53-26	Cu, Ag	Carrizo Mt. Cu, Ag, Zn	Prospect
3104-222-906	Unnamed prospect	N-31-01-43; W-104-53-43	Cu, Ag	Carrizo Mt. Cu, Ag, Zn	Prospect
3104-222-907	Unnamed prospect	N-31-02-27; W-104-54-39	Cu-Ag	Carrizo Mt. Cu, Ag, Zn	Prospect
3104-222-908	Unnamed prospect	N-31-02-27; W-104-53-56	Cu, Ag	Carrizo Mt. Cu, Ag, Zn	Prospect
3104-222-909	Unnamed prospect	N-31-01-45; W-104-52-35	Cu-Ag	Carrizo Mt. Cu, Ag, Zn	Prospect
3104-222-910	Unnamed prospect	N-31-01-17; W-104-53-56	Cu-Ag	Carrizo Mt. Cu, Ag, Zn	Prospect
3104-222-911	Unnamed prospect	N-31-02-29; W-104-54-31	Cu-Ag	Carrizo Mt. Cu, Ag, Zn	Prospect
3104-222-912	Unnamed prospect	N-31-02-17; W-104-53-23	Cu-Ag	Carrizo Mt. Cu, Ag, Zn	Prospect
3104-223-301	Pecos Mine	N-31-13-28; W-104-54-19	Ag, Cu, Pb, Zn	Van Horn-Allamoore Ag, Cu	Abandoned mine
3104-223-302	Eureka Prospect	N-31-14-07; W-104-53-47	Cu, Ag	Van Horn-Allamoore Ag, Cu	Prospect
3104-223-303	Diablo Prospect	N-31-13-15; W-104-54-27	Cu, Ag	Van Horn-Allamoore Ag, Cu	Prospect
3104-223-401	Unnamed prospect	N-31-10-04; W-104-59-26	Gravel	Road metal, borrow pit	Borrow pit
3104-223-501	Marvin-Judson Prospect	N-31-10-00; W-104-55-36	Cu, Ag	Van Horn-Allamoore Ag, Cu	Prospect
3104-223-502	Unnamed prospect	N-31-10-16; W-104-56-17	Cu, Ag	Van Horn-Allamoore Ag, Cu	Prospect
3104-223-503	Unnamed prospect	N-31-10-33; W-104-55-25	Cu, Ag	Van Horn-Allamoore Ag, Cu	Prospect
3104-223-601	Hazel Mine	N-31-10-13; W-104-54-00	Ag, Cu	Van Horn-Allamoore Ag, Cu	Abandoned mine
3104-223-602	Unnamed prospect	N-31-10-10; W-104-54-21	Ag, Cu	Van Horn-Allamoore Ag, Cu	Prospect
3104-223-603	Unnamed prospect	N-31-10-10; W-104-54-13	Ag, Cu	Van Horn-Allamoore Ag, Cu	Prospect
3104-223-701	Garren Ranch Quarry	N-31-07-53; W-104-57-54	Talc	Allamoore Talc District	Active mine
3104-223-702	Anaconda Number 2 Prospect	N-31-08-00; W-104-58-09	Cu	Van Horn-Allamoore Ag, Cu	Prospect
3104-223-801	Unnamed prospect	N-31-09-53; W-104-57-07	Au, Pb, Ag	Van Horn-Allamoore Ag, Cu	Prospect
3104-223-802	Mohawk Mine	N-31-09-44; W-104-57-24	Pb, Ag	Van Horn-Allamoore Ag, Cu	Abandoned mine
3104-223-803	Unnamed prospect	N-31-08-49; W-104-56-33	Au, Ag	Van Horn-Allamoore Ag, Cu	Prospect
3104-223-804	St. Elmo Mine	N-31-08-19; W-104-56-04	Cu, Ag	Van Horn-Allamoore Ag, Cu	Abandoned mine
3104-223-805	Blackshaft Mine	N-31-08-20; W-104-55-29	Cu, Ag	Van Horn-Allamoore Ag, Cu	Abandoned mine
3104-223-806	Hackberry Mine	N-31-08-09; W-104-55-28	Ag, Cu	Van Horn-Allamoore Ag, Cu	Abandoned mine
3104-223-807	Unnamed prospect	N-31-08-14; W-104-55-56	Au, Ag	Van Horn-Allamoore Ag, Cu	Prospect
3104-223-808	Sancho Panza Mine	N-31-08-39; W-104-56-23	Cu, Ag	Van Horn-Allamoore Ag, Cu	Abandoned mine

Appendix II (cont.)

BEG LOCALITY #	NAME	LATITUDE / LONGITUDE	COMMODITY	DISTRICT	TYPE
3104-223-809	Lost Cow Quarry	N-31-07-46; W-104-56-34	Talc	Allamoore Talc District	Active mine
3104-223-901	Tumbledown Mountain Talc Deposit	N-31-08-05; W-104-53-22	Talc	Allamoore Talc District	Active mine
3104-223-902	Prospect 1, 8	N-31-09-52; W-104-54-35	Cu, Ag	Van Horn-Allamoore Ag, Cu	Abandoned mine
3104-223-903	Prospect 15, 16	N-31-08-50; W-104-54-37	Ag, Cu	Van Horn-Allamoore Ag, Cu	Abandoned mine
3104-232-101	Unnamed prospect	N-31-21-49; W-104-59-54	Gravel	Road metal, borrow pit	Borrow pit
3104-232-102	Unnamed prospect	N-31-20-55; W-104-59-22	Gravel	Road metal, borrow pit	Borrow pit
3104-232-901	Unnamed prospect	N-31-15-04; W-104-54-33	Gravel	Road metal, borrow pit	Borrow pit
3105-111-101	Unnamed pit	N-31-07-17; W-105-06-40	Talc	Allamoore Talc District	Prospect
3105-111-102	Unnamed pit	N-31-07-10; W-105-06-45	Road metal	Road metal, borrow pit	Borrow pit
3105-111-103	Unnamed pit	N-31-07-08; W-105-06-52	Road metal	Road metal, borrow pit	Borrow pit
3105-111-201	Unnamed pit	N-31-05-18; W-105-03-18	Road metal	Road metal, borrow pit	Borrow pit
3105-111-202	Unnamed pit	N-31-05-13; W-105-02-40	Road metal	Road metal, borrow pit	Borrow pit
3105-111-203	Unnamed pit	N-31-05-06; W-105-02-44	Road metal	Road metal, borrow pit	Borrow pit
3105-111-301	T & P #1 Quarry	N-31-07-07; W-105-01-52	Talc	Allamoore Talc District	Active mine
3105-111-302	Texola Quarry	N-31-06-47; W-105-01-40	Talc	Allamoore Talc District	Active mine
3105-111-303	Unnamed prospect	N-31-06-26; W-105-00-37	Talc	Allamoore Talc District	Prospect
3105-111-304	Unnamed prospect	N-31-06-38; W-105-00-25	Talc	Allamoore Talc District	Prospect
3105-111-305	Unnamed Quarry	N-31-06-58; W-105-00-06	Talc	Allamoore Talc District	Inactive mine
3105-111-306	Unnamed pit	N-31-06-18; W-105-00-27	Talc	Allamoore Talc District	Prospect
3105-111-307	Unnamed pit	N-31-06-50; W-105-00-19	Talc	Allamoore Talc District	Prospect
3105-111-308	Unnamed pit	N-31-05-06; W-105-02-17	Road metal	Road metal, borrow pit	Borrow pit
3105-111-401	Unnamed pit	N-31-03-31; W-105-05-30	Road metal	Road metal, borrow pit	Borrow pit
3105-111-601	Unnamed pit	N-31-04-50; W-105-01-09	Road metal	Road metal, borrow pit	Borrow pit
3105-111-602	Unnamed pit	N-31-04-35; W-105-00-53	Road metal	Road metal, borrow pit	Borrow pit
3105-111-603	Pit	N-31-04-32; W-105-00-13	Talc	Allamoore Talc District	Active mine
3105-111-604	Unnamed pit	N-31-03-19; W-105-00-31	Road metal	Road metal, borrow pit	Borrow pit
3105-111-605	Unnamed pit	N-31-04-21; W-105-00-50	Road metal	Road metal, borrow pit	Borrow pit
3105-111-901	Unnamed pit	N-31-00-39; W-105-00-54	Road metal	Road metal, borrow pit	Borrow pit
3105-112-301	Unnamed prospects near Eagle Flat	N-31-07-24; W-105-09-46	Ag, Pb, Au	Eagle Flat Prospects Ag, Pb	Prospect
3105-112-302	Lena Mine	N-31-07-16; W-105-08-48	Ag, Pb, Au	Eagle Flat Prospects Ag, Pb	Prospect
3105-112-303	Unnamed pit	N-31-06-54; W-105-09-35	Road metal	Road metal, borrow pit	Borrow pit
3105-112-304	Unnamed pit	N-31-06-39; W-105-08-41	Road metal	Road metal, borrow pit	Borrow pit
3105-112-305	Unnamed pit	N-31-06-26; W-105-07-45	Road metal	Road metal, borrow pit	Borrow pit
3105-112-306	Unnamed pit	N-31-07-14; W-105-10-39	Road metal	Road metal, borrow pit	Borrow pit
3105-112-307	Unnamed pit	N-31-06-48; W-105-08-14	Road metal	Road metal, borrow pit	Borrow pit
3105-113-601	Wilco Claims	N-31-10-19; W-105-07-34	Talc	Allamoore Talc District	Abandoned mine
3105-113-701	Unnamed pit	N-31-08-12; W-105-13-56	Road metal	Road metal, borrow pit	Borrow pit
3105-113-801	Texas Talc Quarry A (Loyce Claims)	N-31-08-51; W-105-10-00	Talc	Allamoore Talc District	Active mine
3105-113-802	Texas Talc Quarry C	N-31-08-53; W-105-10-08	Talc	Allamoore Talc District	Active mine
3105-113-803	Unnamed pit	N-31-07-32; W-105-11-35	Road metal	Road metal, borrow pit	Borrow pit
3105-113-901	Texas Talc Quarry D (Loyce Claims)	N-31-08-49; W-105-09-41	Talc	Allamoore Talc District	Active mine
3105-113-902	Texas Talc Quarry B	N-31-08-38; W-105-09-30	Talc	Allamoore Talc District	Active mine
3105-113-903	Cyprus Minerals Pit	N-31-08-38; W-105-09-01	Talc	Allamoore Talc District	Active mine
3105-113-904	Prospect 5,12	N-31-07-47; W-105-09-14	Ag, Pb	Eagle Flat Prospects Ag, Pb	Abandoned mine
3105-113-904	Unnamed prospect	N-31-07-46; W-105-09-14	Ag, Pb, Au	Eagle Flat Prospects Ag, Pb	Prospect
3105-113-905	Prospect 7,14	N-31-07-32; W-105-09-39	Ag, Pb	Eagle Flat Prospects Ag, Pb	Abandoned mine

Appendix II (cont.)

BEG LOCALITY #	NAME	LATITUDE / LONGITUDE	COMMODITY	DISTRICT	TYPE
3105-113-905	Unnamed prospect	N-31-07-32; W-105-09-37	Ag, Pb, Au	Eagle Flat Prospects Ag, Pb	Prospect
3105-113-906	Prospect 6,13	N-31-07-31; W-105-09-07	Ag, Pb	Eagle Flat Prospects Ag, Pb	Abandoned mine
3105-113-906	Unnamed prospect	N-31-07-30; W-105-09-09	Ag, Pb, Au	Eagle Flat Prospects Ag, Pb	Prospect
3105-113-907	Unnamed Prospect near Lena Tank	N-31-07-42; W-105-07-46	Ag, Pb, Au	Eagle Flat Prospects Ag, Pb	Prospect
3105-114-401	Unnamed pit	N-31-10-25; W-105-07-22	Sand and gravel	Road metal, borrow pit	Borrow pit
3105-114-501	Unnamed prospect	N-31-10-16; W-105-03-21	Talc	Allamoore Talc District	Prospect
3105-114-502	Unnamed prospect	N-31-10-43; W-105-04-17	Talc	Allamoore Talc District	Prospect
3105-114-701	Bill Quarry	N-31-09-53; W-105-05-46	Talc	Allamoore Talc District	Active mine
3105-114-702	Unnamed prospect	N-31-09-48; W-105-05-22	Talc	Allamoore Talc District	Prospect
3105-114-703	Unnamed pit	N-31-09-42; W-105-06-16	Talc	Allamoore Talc District	Prospect
3105-114-704	Rex Quarry	N-31-09-45; W-105-06-31	Talc	Allamoore Talc District	Active mine
3105-114-705	Unnamed prospect	N-31-09-19; W-105-07-04	Talc	Allamoore Talc District	Prospect
3105-114-706	Buck Quarry	N-31-09-15; W-105-06-37	Talc	Allamoore Talc District	Active mine
3105-114-707	Escondido Quarry	N-31-08-44; W-105-05-27	Talc	Allamoore Talc District	Active mine
3105-114-708	Escondido Prospect	N-31-08-44; W-105-05-51	Talc	Allamoore Talc District	Prospect
3105-114-709	Unnamed pit	N-31-08-37; W-105-05-25	Sand and gravel	Road metal, borrow pit	Borrow pit
3105-114-710	Unnamed pit	N-31-09-42; W-105-07-21	Talc	Allamoore Talc District	Prospect
3105-114-801	Pit 1	N-31-08-37; W-105-04-41	Talc	Allamoore Talc District	Abandoned mine
3105-114-802	Unnamed prospect	N-31-08-17; W-105-04-22	Talc	Allamoore Talc District	Prospect
3105-114-803	Pit 4	N-31-08-13; W-105-04-15	Talc	Allamoore Talc District	Abandoned mine
3105-114-804	Dees Quarry	N-31-08-14; W-105-03-15	Talc	Allamoore Talc District	Active mine
3105-114-805	Pit 6	N-31-08-08; W-105-03-18	Talc	Allamoore Talc District	Abandoned mine
3105-114-806	Diablo Prospect, western locality	N-31-09-55; W-105-04-05	Talc	Allamoore Talc District	Prospect
3105-114-807	Diablo Prospect, eastern locality	N-31-09-57; W-105-03-50	Talc	Allamoore Talc District	Prospect
3105-114-808	Unnamed prospect	N-31-09-57; W-105-03-34	Talc	Allamoore Talc District	Prospect
3105-114-809	Unnamed pit	N-31-07-39; W-105-03-00	Talc	Allamoore Talc District	Prospect
3105-114-901	Pit 5	N-31-08-38; W-105-01-50	Talc	Allamoore Talc District	Abandoned mine
3105-114-902	Bobcat Prospect	N-31-08-29; W-105-01-41	Talc	Allamoore Talc District	Prospect
3105-114-903	Unnamed pit	N-31-08-16; W-105-01-40	Talc	Allamoore Talc District	Prospect
3105-114-904	Unnamed prospect	N-31-08-10; W-105-01-35	Talc	Allamoore Talc District	Prospect
3105-114-905	Snow White Quarry	N-31-08-11; W-105-01-01	Talc	Allamoore Talc District	Active mine
3105-114-906	Pink Chips Prospect	N-31-08-06; W-105-00-21	Talc	Allamoore Talc District	Active mine
3105-114-907	Texas Pacific RR Quarry	N-31-07-43; W-105-01-13	Talc	Allamoore Talc District	Active mine
3105-121-101	Unnamed pit	N-31-07-27; W-105-21-11	Road metal	Road metal, borrow pit	Borrow pit
3105-122-101	Quitman Gap Veins (QG-1 and 2)	N-31-05-07; W-105-28-50	Fe	N. Quitman Mts. Ag, Pb, Zn, W, Sn	Prospect
3105-122-102	Cowan Ranch Fluorite Locality	N-31-07-13; W-105-29-39	Fluorspar	N. Quitman Mts. Ag, Pb, Zn, W, Sn	Prospect
3105-122-201	Granite Hill Prospect	N-31-06-40; W-105-26-46	Be, Sn, W, No, Fe	N. Quitman Mts. Ag, Pb, Zn, W, Sn	Prospect
3105-122-401	Red Chief Veins	N-31-04-51; W-105-28-33	Pb, Zn	N. Quitman Mts. Ag, Pb, Zn, W, Sn	Prospect
3105-122-801	Unnamed prospect	N-31-01-13; W-105-26-20	Ag, Au, U	N. Quitman Mts. Ag, Pb, Zn, W, Sn	Prospect
3105-123-101	Unnamed pit	N-31-14-30; W-105-28-50	Sand and Gravel	Road metal, borrow pit	Borrow pit
3105-123-102	Unnamed pit	N-31-12-55; W-105-29-37	Sand and Gravel	Road metal, borrow pit	Borrow pit
3105-123-103	Unnamed pit	N-31-14-59; W-105-29-16	Sand and Gravel	Road metal, borrow pit	Borrow pit
3105-123-201	Unnamed pit	N-31-12-55; W-105-27-20	Ag	N. Quitman Mts. Ag, Pb, Zn, W, Sn	Prospect
3105-123-202	Sierra Blanca Occurrences (South)	N-31-14-09; W-105-25-48	Fluorspar and Beryllium	Sierra Blanca Fluorspar-Beryllium	Occurrence
3105-123-401	Bonanza Mine	N-31-11-13; W-105-30-00	Pb, Ag, Zn	N. Quitman Mts. Ag, Pb, Zn, W, Sn	Abandoned mine
3105-123-402	Love Pass Veins	N-31-11-40; W-105-29-37	Ag	N. Quitman Mts. Ag, Pb, Zn, W, Sn	Prospect

Appendix II (cont.)

BEG LOCALITY #	NAME	LATITUDE / LONGITUDE	COMMODITY	DISTRICT	TYPE
3105-123-403	Milby Peak Vein (MP-1)	N-31-10-57; W-105-27-41	Pb, Zn, Ag	N. Quitman Mts. Ag, Pb, Zn, W, Sn	Prospect
3105-123-404	Tremble Hill Prospect	N-31-10-14; W-105-28-08	Fe, Sn, Be, Cu	N. Quitman Mts. Ag, Pb, Zn, W, Sn	Prospect
3105-123-405	Love Pasture Prospects	N-31-10-40; W-105-29-21	Fe	N. Quitman Mts. Ag, Pb, Zn, W, Sn	Prospect
3105-123-406	Unnamed pit	N-31-12-29; W-105-27-32	Ag	N. Quitman Mts. Ag, Pb, Zn, W, Sn	Prospect
3105-123-501	Bona Prospect	N-31-11-57; W-105-26-56	Ag, Pb, Fe, Ni	N. Quitman Mts. Ag, Pb, Zn, W, Sn	Prospect
3105-123-502	Unnamed pit	N-31-11-57; W-105-26-16	Ag	N. Quitman Mts. Ag, Pb, Zn, W, Sn	Prospect
3105-123-503	Unnamed pit	N-31-10-49; W-105-25-44	Ag	N. Quitman Mts. Ag, Pb, Zn, W, Sn	Prospect
3105-123-504	Tarantula Hills Prospects	N-31-11-21; W-105-27-03	Pb, Ag, Zn, Au, Cu, U	N. Quitman Mts. Ag, Pb, Zn, W, Sn	Abandoned mine
3105-123-505	Unnamed pit	N-31-10-48; W-105-27-09	Cu, Au, Ag	N. Quitman Mts. Ag, Pb, Zn, W, Sn	Prospect
3105-123-506	Milby Peak Vein (MP-2)	N-31-10-42; W-105-27-16	Pb, Zn, Cu	N. Quitman Mts. Ag, Pb, Zn, W, Sn	Prospect
3105-123-507	Stokes Prospect	N-31-11-55; W-105-27-33	Ag, Pb, U	N. Quitman Mts. Ag, Pb, Zn, W, Sn	Prospect
3105-123-601	Unnamed pit	N-31-10-33; W-105-22-38	Sand and gravel	Road metal, borrow pit	Borrow pit
3105-123-801	Unnamed prospect	N-31-09-21; W-105-25-21	uncertain	N. Quitman Mts. Ag, Pb, Zn, W, Sn	Prospect
3105-123-802	Unnamed pit	N-31-09-32; W-105-26-03	uncertain	N. Quitman Mts. Ag, Pb, Zn, W, Sn	Prospect
3105-124-401	Unnamed pit	N-31-11-13; W-105-22-27	Road metal	Road metal, borrow pit	Borrow pit
3105-124-402	Unnamed pit	N-31-10-06; W-105-20-35	Road metal	Road metal, borrow pit	Borrow pit
3105-124-403	Unnamed prospect near Texan Mt.	N-31-10-12; W-105-22-07	Cu	N. Quitman Mts. Ag, Pb, Zn, W, Sn	Prospect
3105-124-404	Unnamed pit	N-31-10-33; W-105-22-25	Cu	N. Quitman Mts. Ag, Pb, Zn, W, Sn	Prospect
3105-124-801	Unnamed pit	N-31-09-48; W-105-19-29	Road metal	Road metal, borrow pit	Borrow pit
3105-124-901	Unnamed pit	N-31-09-06; W-105-17-12	Road metal	Road metal, borrow pit	Borrow pit
3105-124-902	Unnamed pit	N-31-08-42; W-105-15-51	Road metal	Road metal, borrow pit	Borrow pit
3105-124-903	Unnamed pit	N-31-08-30; W-105-15-15	Road metal	Road metal, borrow pit	Borrow pit
3105-132-702	Round Top Prospect	N-31-16-57; W-105-28-46	Fluorspar and beryllium	Sierra Blanca fluorspar-beryllium	Abandoned mine
3105-132-703	Little Round Top Prospects	N-31-17-05; W-105-27-36	Fluorspar and beryllium	Sierra Blanca fluorspar-beryllium	Prospect
3105-132-704	Unnamed pit	N-31-15-04; W-105-28-42	Gravel	Road metal, borrow pit	Borrow pit
3105-132-801	Little Blanca Mountain Prospects	N-31-17-15; W-105-27-06	Fluorspar and beryllium	Sierra Blanca fluorspar-beryllium	Prospect
3105-132-802	Sierra Blanca Occurrences (North)	N-31-15-34; W-105-26-26	Fluorspar and beryllium	Sierra Blanca fluorspar-beryllium	Occurrence
3105-141-301	Unnamed pit	N-31-22-08; W-105-00-17	Gravel	Road metal, borrow pit	Borrow pit
3105-141-501	Unnamed pit	N-31-19-52; W-105-04-23	Gravel	Road metal, borrow pit	Borrow pit
3105-141-801	Unnamed pit	N-31-17-00; W-105-03-12	Gravel	Road metal, borrow pit	Borrow pit
3105-142-601	Unnamed pit	N-31-18-33; W-105-08-59	Sand and gravel	Road metal, borrow pit	Borrow pit
3105-142-701	Unnamed pit	N-31-16-31; W-105-14-47	Sand and gravel	Road metal, borrow pit	Borrow pit